LAWRENCE
LIVERMORE
NATIONAL
LABORATORY

LLNL-TR-750685

Boil-off losses along LH2 pathway

G. Petitpas

May 2, 2018

Disclaimer

This work performed under the auspices of the U.S. Department of Energy by Lawrence Livermore National Laboratory under Contract DE-AC52-07NA27344.

Boil-off losses along the LH_2 pathway

Guillaume Petitpas, Ph.D.

Lawrence Livermore National Laboratory, 7000 East Avenue, Livermore CA 94550

Abstract

Losses along the LH_2 pathway are intrinsic to the utilization of a cryogenic fluid. They occur when the molecule is transferred between 2 vessels (liquefaction plant to trailer, trailer to station storage, station storage to pump or compressor, then fuel cell electric vehicles …) and when the fluid is warmed up due to heat transfer with the environment. Those losses can be estimated with good accuracy using thermodynamic models based on conservation of mass and energy, providing the thermodynamic states are correctly described. Indeed, the fluid undergoes various changes as it moves along the entire pathway (2 phase transition, super-heated warming, non-uniform temperature distributions across the saturation film) and accurate equations of state and 2 phase behavior implementations are essential. The balances of mass and energy during the various dynamics processes then enable to quantify the boil-off losses. In this work, a MATLAB code previously developed by NASA to simulate rocket loading is used as the basis for the LH_2 transfer model. This code implements complex physical phenomena such as the competition between condensation and evaporation and the convection vs. conduction heat transfer as a function of the relative temperatures on both sides of the saturated film. The original code was modified to consider real gas equations of state, and some semi-empirical relationships, such as between the heat of vaporization and the critical temperature, were also replaced by a REFPROP equivalent expression, assumed to be more accurate. Non-constant liquid temperature equations were added to simulate sub-cooled conditions. It is shown that although trailer depressurization and transfer losses from the receiving vessel during a LH_2 delivery may constitute the largest sources of losses, those can be greatly reduced and even eliminated if CFR/DOT regulations are properly applied and if no-vent fill methods are implemented, particularly for a stationary LH_2 storage operating at reasonably low pressure (45 psia or so). As such, it is expected that the only remaining boil-off losses for a refueling station would come from the LH_2 pump (utilization and idling), pump vessel cool down/warm up, and environment heat transfer. Based on experimental data measured at LLNL on the Linde 875 bar LH_2 cryo-pump and results from the model, and extrapolating for refueling stations of various sizes, it can be shown that boil-off losses can vary from 15% of delivered LH_2 for a 100 kg/day, 5% at 400 kg/day, and down to less than 2% for stations above 1,800 kg/day (for a system similar to the one at LLNL). Less boil-off is to be expected for LH_2 pumps dispensing at 350 bar, so that less than 0.7% can be expected above 1,800 kg/day station capacities. At last, boil-off recovery solutions are briefly analyzed, including compressors, cryo-coolers and stationary fuel cell. Their economic value is strongly related to the costs of H_2 and of the electricity needed to perform the recovery, on top of the initial capital expenditures. Effective boil-off could be reduced to 0.6-1% for a 2,000 kg/day station if adequate recovery solutions are used.

Final Version: July 2018, External Audience (Unlimited)

Table of Contents

List of Figures

List of Tables

Introduction

Liquid hydrogen (LH_2) has many benefits for the hydrogen infrastructure: its high density allows minimum costs for distribution (e.g. \$167/kg H_2 for a liquid trailer vs. \$783/kg H_2 for a gaseous trailer [1]) and stationary storage, its high payload and short transfer times ease delivery logistics, its low temperature provides very low potential burst energy [2], and LH_2 pumps can efficiently achieve large throughputs at the refueling stations with a small footprint (low electricity consumption and compact designs).

Those benefits translate into significant capital and operational expenses reduction for hydrogen refueling station owners and operators. For example, **Figure 1** shows the initial installed capital expenditure for various 4,000 kg/day hydrogen refueling station designs: the first 3 rely on LH_2 delivery, while the last 2 rely on gaseous delivery. All assume gaseous ambient 350 bar storage onboard the Fuel Cell Electric Vehicles – FCEV (capacity: 50 kg), except the first one ("CcH_2" or cryo-compressed H_2 [3],[4]) that assumes cryogenic storage at 350 bar. As such, the fuel is directly dispensed to the FCEV (no cascade, no evaporator). Also, the first two scenarios (from the left) use a LH_2 pump, and the third scenario uses a compressor that vaporizes the LH_2 before compressing it. The major cost differences come from the cost of the LH_2 pump vs. compressor (red bars) and the bulk storage (blue bars). Please note that the outcomes from the model [5] have been slightly modified for the fourth scenario: the cost of the gaseous delivery tube trailer(s) was added to the "bulk storage" cost as such a large station would need to have trailers dedicated only to that station. **Figure 2** highlights the cost difference of installed compressors and LH_2 pumps in \$2016/(kg/hour) for 3 different production volume assumptions (low, mid and high). At 350 bar, compressors are 2.7 times more expensive than LH_2 pumps to achieve the same throughput. This ratio becomes 3.4 at 700 bar.

The benefits of LH_2 distribution are illustrated in a California Air Resources Board (CARB) report [6], that analyses future deployment of H_2 fueling stations for different sources of H_2 (liquid or gaseous delivery, or on-site SMR). CARB anticipates that, regardless of the rate of FCEV introduction, most fueling stations will be supplied with LH_2 in the future. Indeed, LH_2 distribution is particularly favorable as station size/utilization increases. For example, the largest fleet of H_2 buses in the world (AC Transit [7] in Oakland, CA) uses LH_2, and most of the ~40 FC forklift refueling stations in the U.S. are relying on LH_2 supply.

Using LH_2 has a few challenges: liquefying H_2 is expensive (more than 3 times the energy of compression to 700 bar [8]), setback distances are more stringent for LH_2, and boil-off losses along the LH_2 pathway may occur. LH_2 losses are not well qualified nor quantified, and more analysis needs to be performed to evaluate their impact on the hydrogen cost. This report addresses this lack of understanding by developing a simulation framework for LH_2 transfer between tanks (also including heat transfer with environment) using real gas equation of states and physical models for the interaction between the 2 phases and the saturation film, based on the work by Osipov *et al* [9], [10], initially performed for the simulation of LH_2 rocket loading. The LH_2 pathway considered in this work is presented in Section 1, including specifications of the volume, capacity and pressure ratings of the vessels along the pathway. Section 2 describes the modeling framework that was used, and the modifications made to the original code. Section 3 presents the main results from the modelling effort. Section 4 analyses strategies to reduce the boil-off during LH_2 transfer at the station. Section 5 summarizes a typical boil-off budget for station sizes ranging from 100 to 6,000 kg/day. Section 6 analyses boil-off recovery solutions that may be implemented.

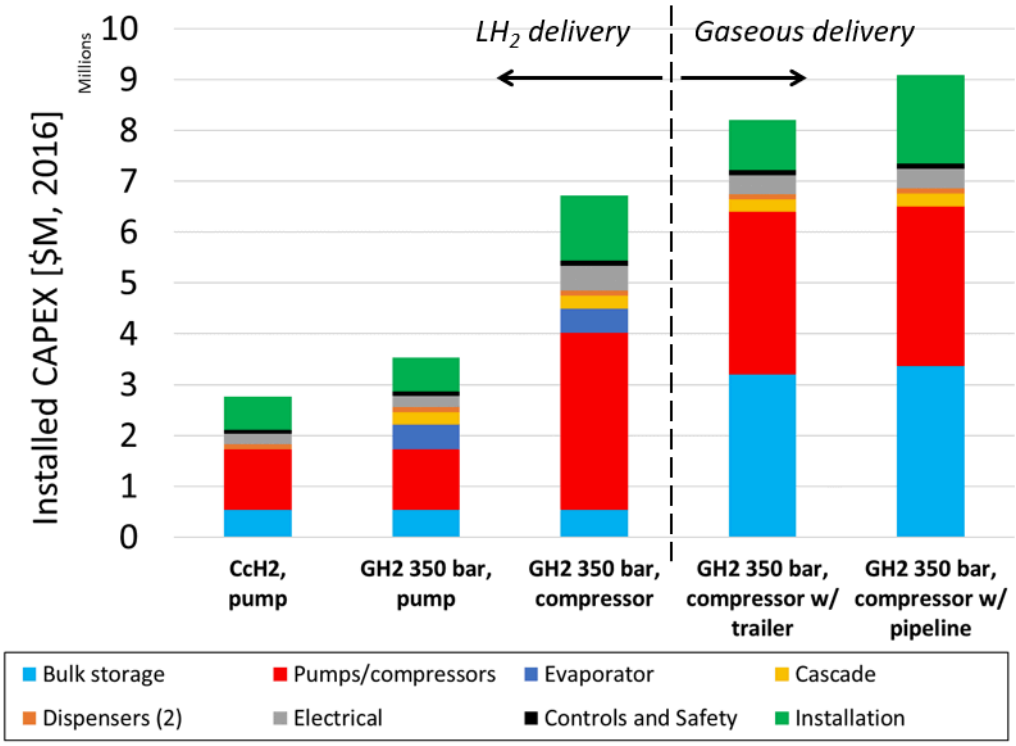

Figure 1: Projected installed capital expenditures in $2016, for a 4,000 kg/day hydrogen refueling station (FCEV capacity: 50 kg H_2) computed from HDRSAM V1.0 [5], assuming high production volume.

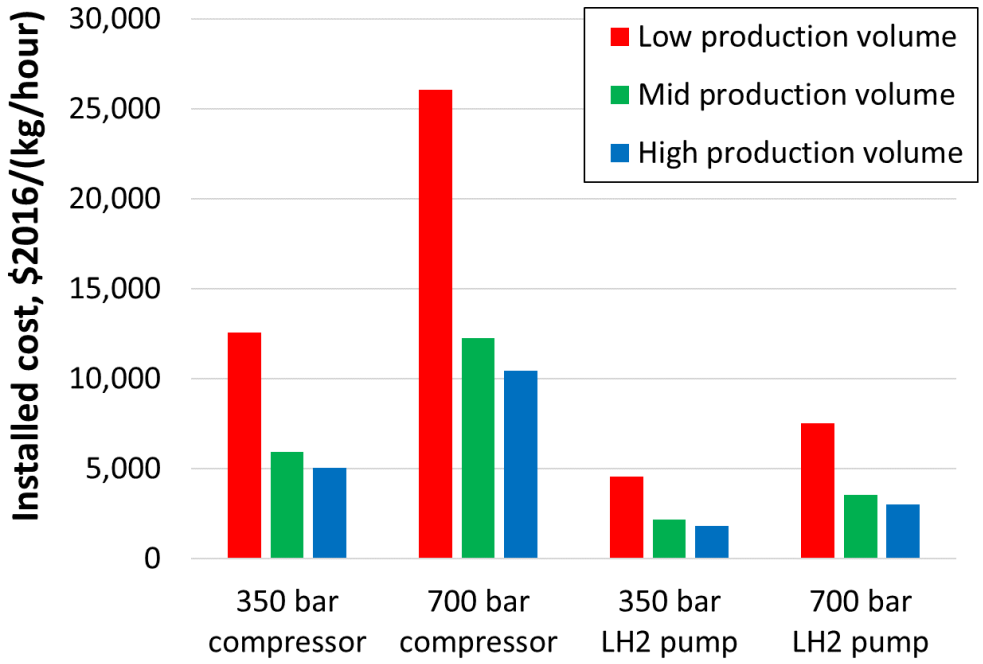

Figure 2: Projected installed cost of 350 and 700 bar compressors and LH_2 pumps in $2016/(kg/hour), as computed from HDRSAM V1.0 [5], for different production volumes (low, mid and high). Compressors are 5 stages with a 3 bar suction pressure. Flow rates for compressors and LH_2 pumps are 35 and 120 kg/hour, respectively.

1. Description of the LH_2 pathway

The LH_2 pathway considered in this study consists of a liquid terminal at the liquefaction plant, a liquid trailer that ships LH_2 from the liquid terminal to the refueling station, and the stationary storage at the refueling site. Size and ratings of the equipment can vary, and the specific values of existing equipment considered as baseline for this study are reported in **Table 1**. The liquefaction plant is owned by Praxair and located in Ontario, CA. It is a 30 US tons per day plant producing LH_2 from natural gas via on-site steam reforming. LH_2 is transferred onto the trailer directly from the outlet of the liquefier or from the 100 US tons storage, both being operated at similar pressures.

Table 1: Size and ratings of the LH_2 pathway apparatuses. The units used here match the nameplate for each equipment, to facilitate comparison. Therefore, values are given in English units.

	Water volume, gallons	**Max H_2 capacity, lbs.**	**Rated pressure, psig**	**Range of operating pressure, psig**
Storage at liquefaction plant (Praxair, Ontario, CA)	300,000	192,000	15	8 to 10 psig
LH_2 trailer (Linde, #7016)	17,000	8,400	175	Before fill @ plant: 2 to 4 psig Before delivery @ station: 50 to 60 psig
Storage at H_2 station (Livermore, CA)	3,300	1,800	175	30 psig
Pump vessel, 875 bar Linde LH_2 pump (Livermore, CA)	100 L (80 L effective)	~ 12	75	30 psig

Prior to being refilled, the LH_2 trailer vents its remaining H_2 that is recirculated through the liquefaction plant until it reaches 2 to 4 psig. The refill process takes 3 to 6 hours and is monitored using a weighing scale on which the trailer is parked. During the refill process, any vented H_2 is recirculated back the liquefaction plant. Once filled, the trailer then departs to deliver its payload. At the station, the trailer is first pressurized using the vaporizer to reach a vapor pressure above the pressure in the stationary storage, by at least 20 psi or so. If the pressure in the stationary storage is too high, it is vented away to enable delivery. Some H_2 from the trailer is then used to purge and pre-cool the transfer lines and valves. During LH_2 delivery, the vaporizer from the trailer is used to maintain constant pressure differential and enable flow. An indicator called "tricock" is used to monitor the level of fill during the delivery, that is stopped once the liquid H_2 reaches the maximum capacity of the stationary vessel (usually 80 to 90% of the total water volume). At least 2 techniques are used to measure the total amount of H_2 delivered from the LH_2 trailer to the stationary storage: either the entire trailer's mass is measured before and after the delivery using a scale, either a LH_2 meter installed onboard the trailer is used. Those 2 techniques may show discrepancies depending on their accuracies and the amount of vapor H_2 that is vented at the end of the LH_2 delivery. Also, scales may have resolution as high as 20 lbs. At last, the "scale approach" should account for the variation of total mass due to the fuel being consumed by the truck between two measurements.

The LH_2 from the stationary storage is then used to fill vehicles. Different options exist to pressurize the H_2 to conditions suitable for dispensing. LH_2 can either be vaporized then compressed onto buffer storage vessels (=cascade), it can be pressurized using a LH_2 pump then vaporized and stored into a cascade, or it can be directly pressurized towards the FCEV, using a vaporizer in between depending whether the storage system onboard the vehicle is insulated or not. This work is focused on the case of direct refueling of an insulated pressure vessel (also known as "cryo-compressed" [3],[4]) storage system using a LH_2 pump, i.e. without vaporizer nor a cascade between the pump and the vehicle's storage.

2. Dynamical transfer model

The model used in this study is based on the work by Osipov *et al* ([10], [11], [12],[13]) on the modelling and simulation of rocket propellant loading using LH_2. The MATLAB code that was implemented to perform the simulations was published as open-source (NASA technical report 216394, [12]) and used as a baseline for this study.

The code uses dynamic equations to model the complex heat transfer modes that take place during the dynamic process: conduction vs. convection between the saturated film and the vapor/the liquid, condensation and evaporation, energy balance. Ideal gas equations of state are used to describe the thermodynamic states of hydrogen. An overall description is first given in the next section then modifications brought to the original code are presented.

2.1. Overall description of the original code

By employing basic conservation laws, the reduced lumped-parameter model takes into consideration the major multiphase mass and energy exchange processes involved, such as highly nonequilibrium condensation–evaporation of hydrogen, pressurization of the tanks, and liquid hydrogen and hydrogen vapor flows. A self-consistent theory of dynamical condensation–evaporation has been developed that incorporates heat flow by both conduction and convection through the liquid/ vapor interface inside the tanks. A simulation has been developed in MATLAB for a generic refueling system that involves the solution of a system of ordinary integro-differential equations.

Governing mass and energy balances for a 2-phase cryogenic storage system are illustrated in **Figure 3** (left and right, respectively). The vessel's wall, of mass m_{wall},is assumed to have a uniform temperature T_{wall}. The volumes of vapor and liquid H_2 have masses, temperature and pressures denoted by subscripts $_v$ and $_l$, respectively. The saturation film is assumed to be mass-less, with a temperature T_s. Green arrows represent the flows of H_2 entering/leaving the vessel, blue arrows represent the condensation and heat transfer with the saturation film, and red arrows represent the heat transfer for the vessel's wall (environment to the wall Q_{EW}, and wall to liquid and vapor, Q_{WV} and Q_{WL} respectively).

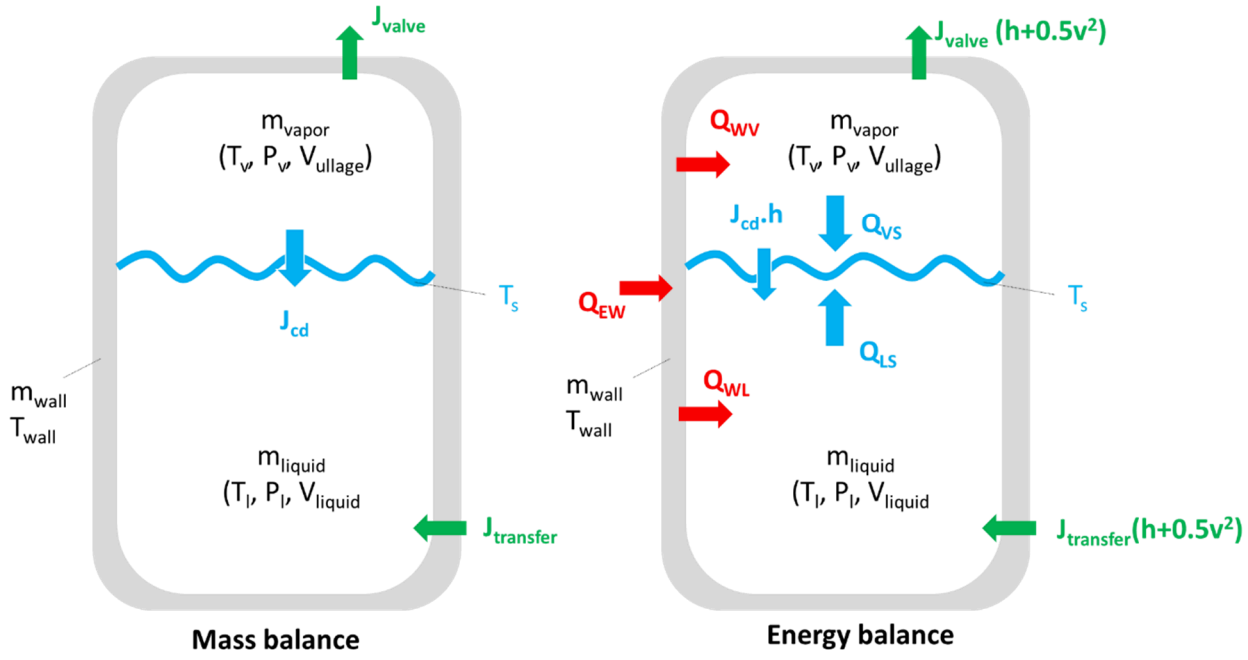

Figure 3: Illustration of the conservations of mass and energy for a 2-phase cryogenic pure fluid. Subscripts $_v$ and $_l$ stand for vapor and liquid, respectively.

The conservation of mass for the liquid and vapor are written as follows:

$$\frac{dm_L}{dt} = \mathrm{J_{cd}} + \mathrm{J}_{transfer} \qquad (1)$$

$$\frac{dm_V}{dt} = -\mathrm{J_{cd}} - \mathrm{J_{valve}} \qquad (2)$$

$\mathrm{J_{transfer}}$ is the mass flow of liquid H_2 entering the liquid volume. $\mathrm{J_{valve}}$ is the flow of vapor leaving the vapor volume. $\mathrm{J_{cd}}$ is the flow of condensing vapor: if positive, some vapor condenses and become liquid; if negative, some liquid boils and becomes vapor. This term is governed by the heat transfer from both the vapor and liquid volumes as:

$$\mathrm{J_{cd}} = -\frac{Q_{LS} + Q_{VS}}{q_{heat\ of\ vaporization}} \qquad (3)$$

Q_{LS} and Q_{VS} are the heat transfer from the liquid, respectively vapor, to the saturated film, in Watts. The denominator is the heat of vaporization, in J/kg.

$\mathrm{J_{transfer}}$ is calculated based on the difference of total pressure between a feeding and a receiving vessel, noted 1 and 2 respectively, such as:

$$J_{transfer} = 2\pi\left(\frac{D}{2}\right)^2 \sqrt{\frac{2\rho_1\left(P_{total,1} - P_{total,2}\right)}{\alpha}} \quad (4)$$

Where D is the diameter of the main valve in the transfer line, α is the corresponding valve coefficient, ρ1 is the density of the hydrogen in the transfer line (assumed to be equal to the liquid density in the feeding vessel 1), and P_{total} is the total pressure (vapor + liquid pressure) for each vessel.

J_{valve} is calculated using choked flow equations based on the ratio between the vapor pressure and the downstream pressure, usually atmospheric pressure.

The conservation of energy of the liquid and the vapor are written as:

$$\frac{d(m_L.u_L)}{dt} = Q_{WL} - Q_{LS} + pdV + J_{cd}.h + J_{transfer}.\left(h + \frac{v^2}{2}\right) \quad (5)$$

$$\frac{d(m_V.u_V)}{dt} = Q_{WV} - Q_{VS} - pdV - J_{cd}.h - J_{valve}.\left(h + \frac{v^2}{2}\right) \quad (6)$$

The terms *h* and *v* are used are generic terms for enthalpy and velocity. Each term is estimated at the conditions of interest (saturated film, feeding vessel and vapor, respectively). The velocity *v* is calculated as the ratio of the flow rate time the density divided by the surface area at the opening.

For the vessel's wall, the conservation of energy is:

$$m_{wall}\frac{d(c_{wall}.T_{wall})}{dt} = Q_{EW} - Q_{WL} - Q_{WV} \quad (7)$$

C_{wall} is the heat capacity of the wall and is temperature-dependent (see section 2.2.4 for details).

The processes of heat transfer, thus the computation of the terms Q_{LS} and Q_{VS}, and phase change prove to be central to the understanding of the loading system and its correct functioning [14] [15]. In [14] , Estey et al. took into consideration heat transfer by convection only while describing a cryogenic (external) tank history. In some cases, however, the heat transfer by conduction is essential in the treatment of the heat and mass flow across the LH_2/GH_2 boundary leading to the so-called condensation blocking [11].

If in a tank partially filled with low pressure cryogenic fluid, the liquid phase is in thermodynamic equilibrium with the vapor phase above it, then the temperature profile is uniform across the interface. The mass flow rate due to condensation J_{cd} is balanced by the evaporation mass flow rate J_e so that both the net mass flow rate $J_{lv}=J_{cd}-J_e$ from the vapor control volume (CV) to the liquid CV and the heat flow through the liquid/vapor interface both disappear. When the tank is being filled or emptied, $J_{lv} \neq 0$. As evaporation

is accompanied by heat removal, it leads to cooling of the interface, while condensation results in its heating. Therefore, in nonequilibrium conditions the interface temperature T_S differs from that of the bulk liquid T_l and that of the vapor T_v, resulting in temperature gradients in both the liquid and vapor volumes adjacent to the interface, as shown in Figure 4, in which possible operational modes are indicated that can be responsible for the shown sequence of temperatures. J_{le} and J_{ve} are external flow rates corresponding to mass leaving the liquid and vapor control volumes, respectively. In turns, these gradients will generate heat fluxes across the interface. Depending on the situation, these fluxes can be associated with heat transfer due to conduction or natural convection [11]. Estimates [12] show that if the processes involved vary slowly over timescales exceeding 0.1 s, then the natural convection, if present, dominates the heat conduction in vapor CV at low temperatures. The heat transfer from the tank walls will further facilitate the effect of convection. Then, taking into consideration that natural convection can occur if the lower part of a CV (liquid or vapor) is hotter than the upper one, the classification of temperature gradients and of the heat transfer regimes in the vicinity of the liquid/vapor interface can be seen in **Figure 4**.

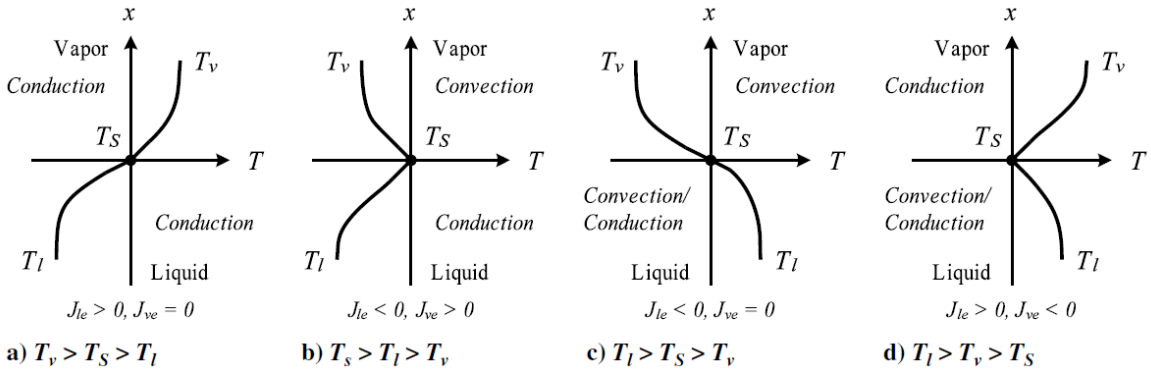

Figure 4: Heat exchange modes at the liquid/vapor interface in the LH_2 tank, reproduced from [10] (not subject to copyright protection in the United States) . T_l, T_S, and Tv stand for liquid, saturation and vapor temperatures, respectively. J_{le} and J_{ve} are external flow rates corresponding to mass leaving the liquid and vapor control volumes, respectively.

The net condensation–evaporation mass flow through the interface is associated with the latent heat generated at, or absorbed by, the interface. Taking into account the microscopic Hertz–Knudsen relation [16] for the condensation–evaporation fluxes, it is possible [11] (1) to relate the interface temperature to the vapor pressure and (2) to prove that the pressure at the LH_2/GH_2 interface is close to that of saturated LH_2 vapor taken at the interface temperature T_S. In other words, in spite of highly nonequilibrium conditions in the tank, quasi equilibrium takes place at the LH_2/GH_2 interface as a result of the so-called dynamical condensation blocking effect [11]. It can be explained as follows. Because of LH_2's low thermal conductivity, the LH_2/GH_2 interface temperature, depending on the situation, either rises or drops due to the condensation–evaporation latent heat released or absorbed at the interface until the condensation mass flow rate nearly compensates the evaporation mass flow rate. These considerations allow to introduce a very thin, massless, saturated vapor film CV (*f*) that separates the vapor CV from that of the liquid (see also Estey et al. [14]). The temperature across this thin film T_f is considered uniform and set to be equal to T_S.

2.2. Modifications to the existing code

2.2.1. Real gas equations of state

Using real gas equations of state in 2 phase conditions is important to make sure the thermodynamics states are accurately described. For example, using the ideal gas law PV=nRT assumes linearity between pressure and temperature, which is inaccurate in the two-phase region. Similarly, using approximations based on the specific heat of constant volume or pressure in order to calculate internal energy or enthalpy can lead to important discrepancies, as illustrated in **Figure 5** where the saturated vapor and liquid enthalpies calculated either the ideal gas law or a real equation of state (here: 32 term modified Benedict-Webb-Rubin equations of state from [17]) are compared.

The original MATLAB code was modified to consider real gas equations of state and transport properties, that were implemented by linking to the MATLAB code to a REFPROP (Version 9.1 [17]) subroutine [18]. REFPROP (REFerence fluid PROPerties) is a thermodynamic database developed by the National Institute of Standards and Technology that implements three models for the thermodynamic properties of pure fluids: equations of state explicit in Helmholtz energy, the modified Benedict-Webb-Rubin equation of state, and an extended corresponding states (ECS) model. Mixture calculations employ a model that applies mixing rules to the Helmholtz energy of the mixture components; it uses a departure function to account for the departure from ideal mixing. Viscosity and thermal conductivity are modeled with either fluid-specific correlations, an ECS method, or in some cases the friction theory method.

Additionally, the energy equations were modified so that variations of internal energies, and not temperature, are used for computing conservation of energy.

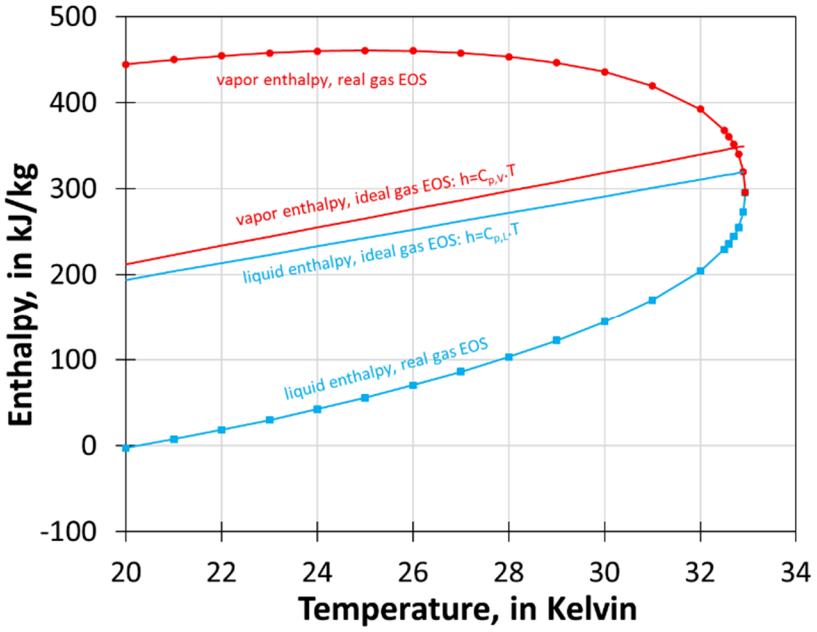

Figure 5: Comparison of the saturated vapor and liquid enthalpies calculated using either ideal gas or real gas equations of state. Enthalpy and entropy reference states are defined at Normal Boiling Point conditions, for the molecule of para-hydrogen.

2.2.2. Non-constant liquid temperature

The original code assumed that the bulk temperature of the liquid phase remained constant (=20 K). Conservation of energy equations were added for both feeding and receiving vessels in order to simulate variations of temperature in the bulk liquid phases.

2.2.3. Top fill

The option of filling a vertical cryogenic tank with LH_2 through from the top was also added to the original code. The underlying physics of the evaporation of a LH_2 droplet inside cryogenic vapor H_2 environment are rather complex. Instead, it was chosen to consider a rather simple approach where only a fraction of the LH_2 being fed at the top of the receiving vessel would evaporate and participate into the mass and energy balances for the vapor CV. As a result, a fraction term was added to the conservation of mass and energy such as equations (1), (2), (5) and (6) become:

$$\frac{dm_L}{dt} = \mathrm{J_{cd}} + \left(1 - X_{top}\right).\mathrm{J}_{transfer} \tag{8}$$

$$\frac{dm_V}{dt} = -\mathrm{J_{cd}} - \mathrm{J_{valve}} + X_{top}.J_{transfer} \tag{9}$$

$$\frac{d(m_L.u_L)}{dt} = Q_{WL} - Q_{LS} + pdV + \mathrm{J_{cd}}.h + \left(1 - X_{top}\right).\mathrm{J}_{transfer}.\left(h + \frac{v^2}{2}\right) \tag{10}$$

$$\begin{aligned}\frac{d(m_V.u_V)}{dt} = {} & Q_{WV} - Q_{VS} - pdV - \mathrm{J_{cd}}.h - \mathrm{J}_{valve}.\left(h + \frac{v^2}{2}\right) \\ & + X_{top}.\mathrm{J}_{transfer}.\left(h + \frac{v^2}{2} - h_{vaporization}\right)\end{aligned} \tag{11}$$

Where X_{top} is the fraction of LH_2 flowing at the top of the receiving vessel, and $h_{vaporization}$ is the enthalpy of vaporization.

2.2.4. Tank thermal mass

The code was initially written assuming a constant thermal inertia (in J/K) for the specific heat of the vessel's wall. This term was modified to consider the actual mass of our stationary Dewar and a temperature dependency for the specific heat capacity. The stationary Dewar that was modeled in this analysis was manufactured in 1991 by Airco Gases and Welding, with a 3,300 gallon inner capacity (12.5 m^3) and an inner vessel made of SA240 T304 with a calculated mass of 2,513 kg (based on geometry and thickness). The temperature dependent specific heat expression for stainless steel 304 was taken from [19], with a 3 to 300 K data range – see **Figure 6**. It was assumed that the rest of the vessel (insulation material, outer shell) was not contributing to the energy balance.

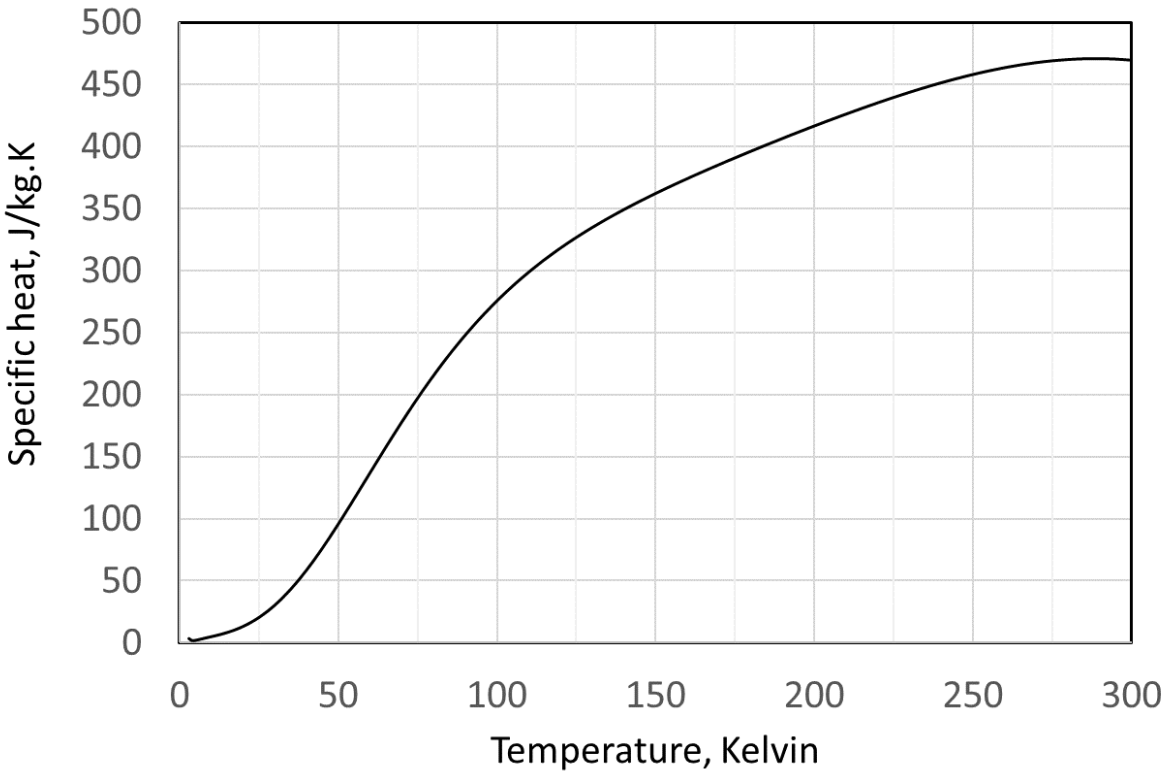

Figure 6: Temperature dependent specific heat of stainless steel 304, from [19]

2.3. Additional assumptions

A few additional assumptions used to simulate the LH_2 transfer with the code are summarized below.

First, the code is 0 D (quasi-dimensional). No temperature distribution (besides through the boundary layers on both sides of the saturation film) is considered. Additionally, no volume nor mass of H_2 in pipes is taken into account. There is no pressure drops through the pipes, nor heat loss or "hot spot" (perfect insulation).

The vessel's wall is considered at uniform temperature.

It is assumed that the trailer is used regularly enough and that its bulk fluid temperature is rather low and constant. As a result, no thermal mass for the trailer's wall is considered.

At last, no para-ortho conversion is considered (H_2 is almost all para), justified by the typically low temperatures and pressures, and the relatively short times.

3. Results from the modified simulation code, applied to LH_2 pathway

In this section we present the results from the simulation code for different situations along the LH_2 pathway. Calibration and verification runs were first performed in order to use the adequate heat input to the vessels, by comparing measured vs. simulated boil-off, and also to make sure that the effective diameters of the pipes and valves allowed for transfer time similar to the ones observed in reality (~30 minutes for the fill of the 3,300 gallon Dewar, 3 to 6 hours for the LH_2 trailer at the plant). Transfer at the LH_2 terminal between the liquefier and the LH_2 trailer were simulated, but the transfer losses were not considered for the overall losses budget, since it was assumed that they were recycled at the liquefaction plant

3.1. Calibration and verification runs

3.1.1. Boil-off from the 3,300 gallon Dewar under heat transfer with environment only (static)

The 3,300 gallon Dewar was installed at Lawrence Livermore National Laboratory (Livermore, CA) in July 2013, and variations of the LH_2 inventory measured in "inH_2O" have been recorded at an hourly rate. Those variations can be used to calibrate/verify the simulations for a vessel filled with LH_2 and subject to heat transfer with environment only ("static" conditions).

The relationship between the indicated level, in inH_2O, and the volume of liquid, in gallons, is shown on the calibration report in Appendix A. **Figure 7** shows variations of volume of LH_2 of an undisturbed (no mass variations other than boil-off from heat transfer with environment) 3,300 gallon Dewar whose relief pressure device is set at 45 psia. 5 different periods are shown: three recorded in the Winter, one recorded in Fall and one in the Summer. At high volume capacities, the boil-off rate looks independent of the season, while the effect of different outside temperatures is noticed at volumes below 1,700 gallons. Additionally, the rate of boil-off does not appear to be constant across the range of volumes: the rate of change decreases with the level of LH_2 in the vessel. Note that the transducer seems to have resolution or linear issues below 1,000 gallons. Also shown on the figure are results from the model for different constant heat transfer assumptions between the 3,300 gallon Dewar wall and the environment (black dotted lines, heat transfer between 30 and 70 Watts). The model predicts linear variations of the volume of LH_2 for a constant heat transfer. Using those results, the variations of the heat transfer as a function of LH_2 volume can be estimated using a polynomials correlation. **Figure 8** shows the estimated heat transfer profile for a 3,300 gallon Dewar for the 2 most extreme recorded conditions (Summer and Winter 2015), with heat transfer between 30 Watts when empty (but still cold) and 70 Watts when filled up to the tricock (=3,000 gallons, 90% full). Assuming a 29 m^2 surface area for the inner vessel, the insulation performance is thus estimated to be between 1 and 2.5 W/m^2.

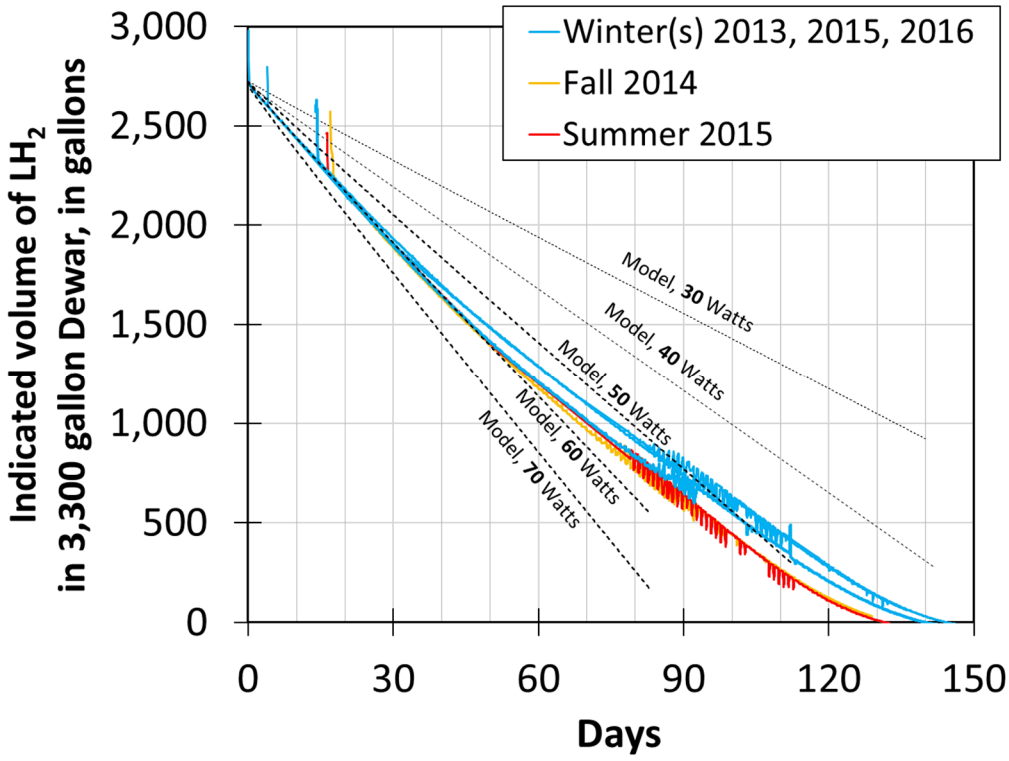

Figure 7: Variations of LH_2 volumes measured for the 3,300 gallon Dewar over different seasonal timeframes with a relieve set pressure of 45 psia, obtained at Lawrence Livermore National Laboratory (Livermore, CA), Winter seasons have similar behaviors. Fall 2014 and summer 2015 show slightly faster boil-off, especially at volumes below 1,700 gallons. Results from the model with constant heat transfers between 30 and 70 watts are also represented, in black dotted lines.

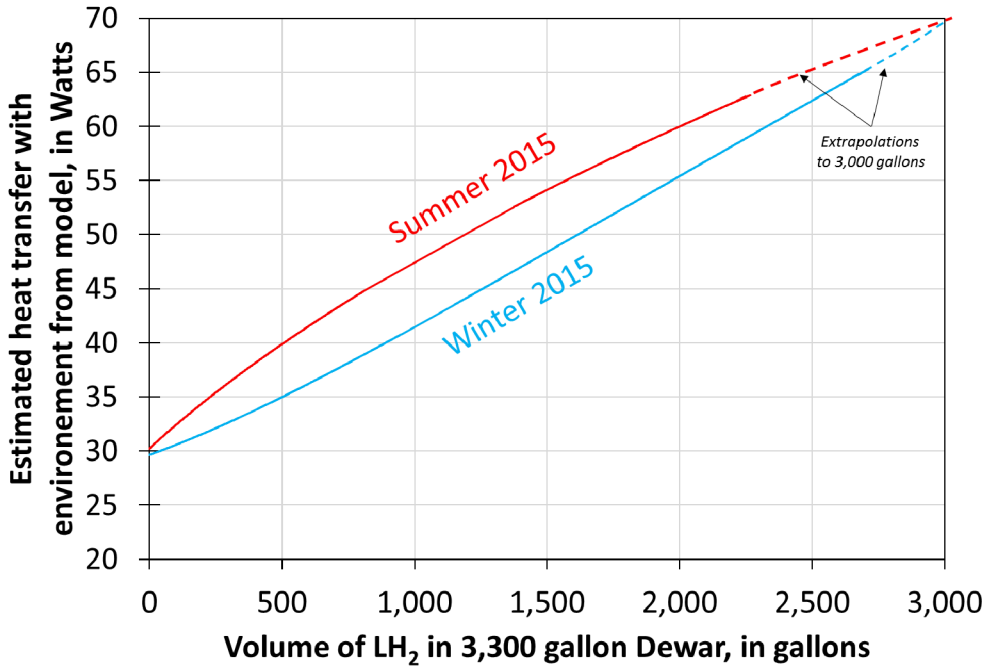

Figure 8: Estimated heat transfer profile between the H_2 and the environment for the 3,300 gallon Dewar. The heat transfer appears to be a strong function of the level of LH_2. Best and worst-case scenarios are shown (Summer and Winter 2015).

Figure 9, **Figure 10** and **Figure 11** show results from the model, simulated for a tank initially filled with 3,000 gallons LH_2 at 20 psia and 21 K (uniform temperature distribution), and exposed to the heat transfer with the environment shown in Figure 8 ("Summer 2015"). The set pressure relief device is 45 psia.

Temperatures variations are shown on **Figure 9**. It takes about 6 days to go from 20 to the maximum pressure (45 psia). After that, the temperature of the saturated film remains constant (24.7 K) since it is controlled by the constant vapor pressure. The liquid phase is warmer than the saturated film and decreases as the tank empties. The vapor temperature continuously increases (26 to 27 K), and so does the vessel's wall temperature.

The heat transfer variations in **Figure 10** enable to better understand the temperature variations for the liquid (left) and vapor (right) phases. On both plots, the black line is the total heat transfer to each phase, based on equations (5) and (6). We can see that most of the heat transfer from the environment (through the wall, thus terms Q_{WL} and Q_{WV}) goes to the liquid phase. However, because of the saturation temperature being lower than the liquid temperature ($-Q_{LS}$) and the cooling due to evaporation ($-J_{cd}.h$), the liquid phase experiences negative to zero het transfer. Conversely, the vapor phase receives most of the heat transfer, mostly due to the evaporation.

At last, variations of LH_2 volume and density can be seen on **Figure 11**. The LH_2 volume first increases within the first 6 days, since the liquid volume heats up, thus lowers its density. It reaches a value near the water volume of the vessel (3,300 gallons), which is rather unusual for a cryogenic pressure vessel. Most of the time, liquid volume never exceeds 85 to 90% of the maximum capacity. Under those conditions, a maximum capacity of 789 kg H_2 (up to 788 kg LH_2) is reached. As such, 90% of that value, i.e. 710 kg LH_2, is considered as a reasonable upper capacity of the 3,300 gallon vessel. The figure also shows that the LH_2 density reaches a low value of 63.2 g/L (after boil-off venting starts) and only slightly increases during boil-off, without ever reaching its saturated value at 45 psia (64.92 g/L). Therefore, the set relief pressure is not seen as an accurate indicator of the actual density of LH_2 inside a Dewar.

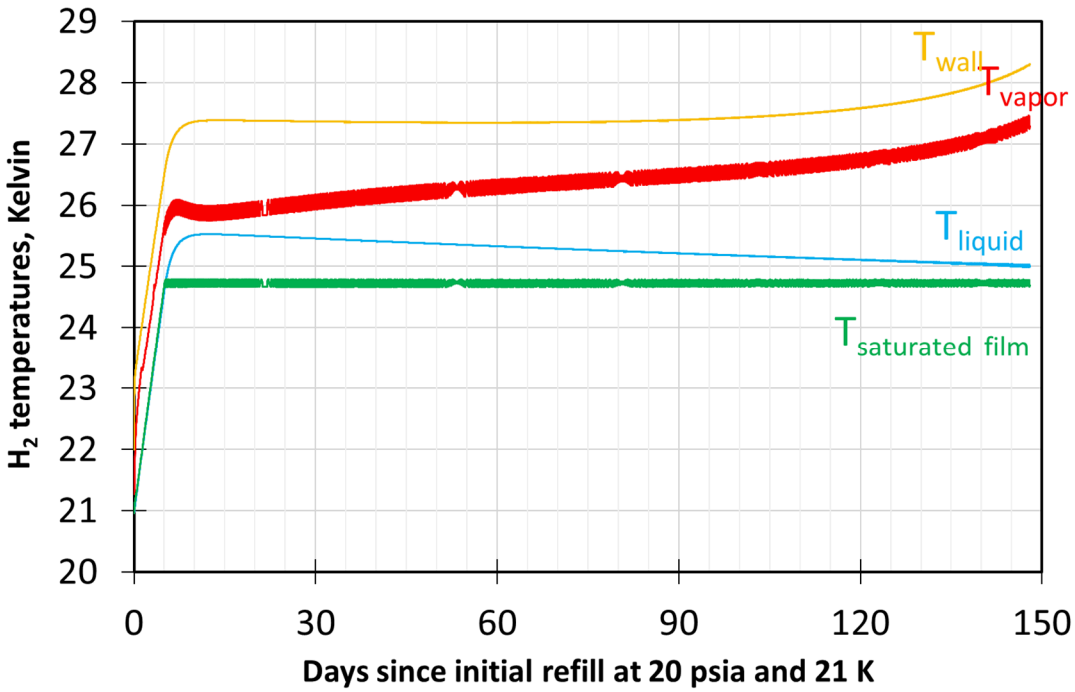

Figure 9: Variations of temperatures (wall, vapor, liquid, and film) for a 3,300 gallon Dewar with a 45 psia set pressure relief and exposed to the heat transfer with the environment shown in **Figure 8** ("Summer 2015"). The tank is initially filled with 3,000 gallons LH_2 at 20 psia and 21 K (uniform temperature distribution). Results computed with MATLAB code.

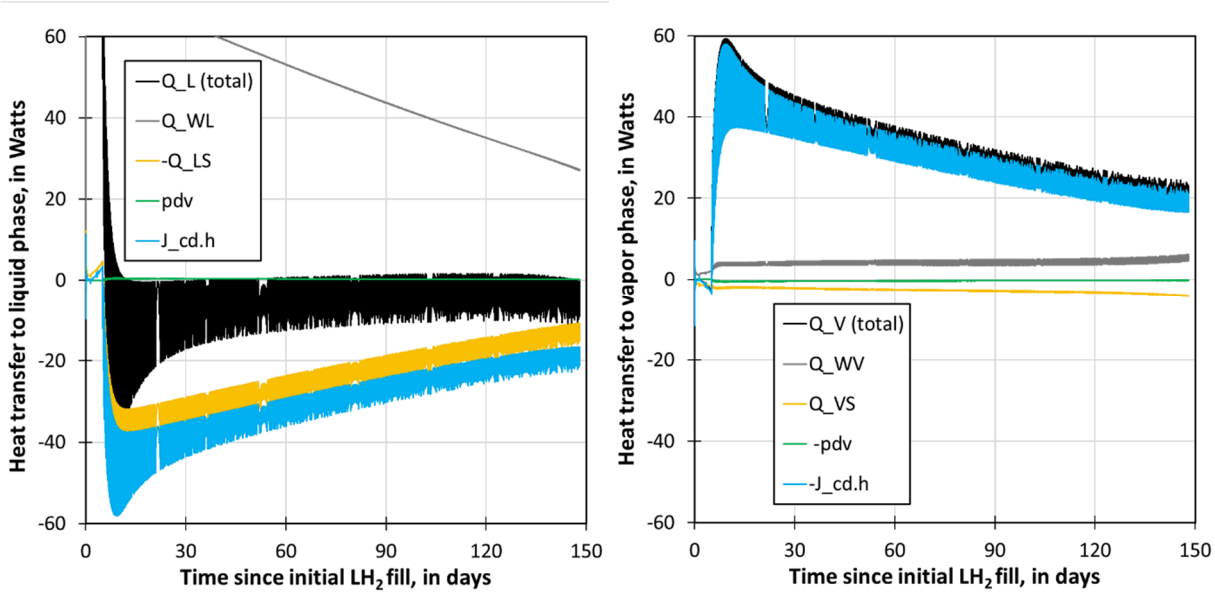

Figure 10: Heat transfer to liquid (left) and vapor (right) phases for a 3,300 gallon Dewar with a 45 psia set pressure relief and exposed to the heat transfer with the environment shown in **Figure 8** ("Summer 2015"). The tank is initially filled with 3,000 gallons LH_2 at 20 psia and 21 K (uniform temperature distribution). "Q_L (total)" and "Q_V (total)" represent the total heat transfer to each phase (left hand side term in equations (5) an (6)). Results computed with MATLAB code.

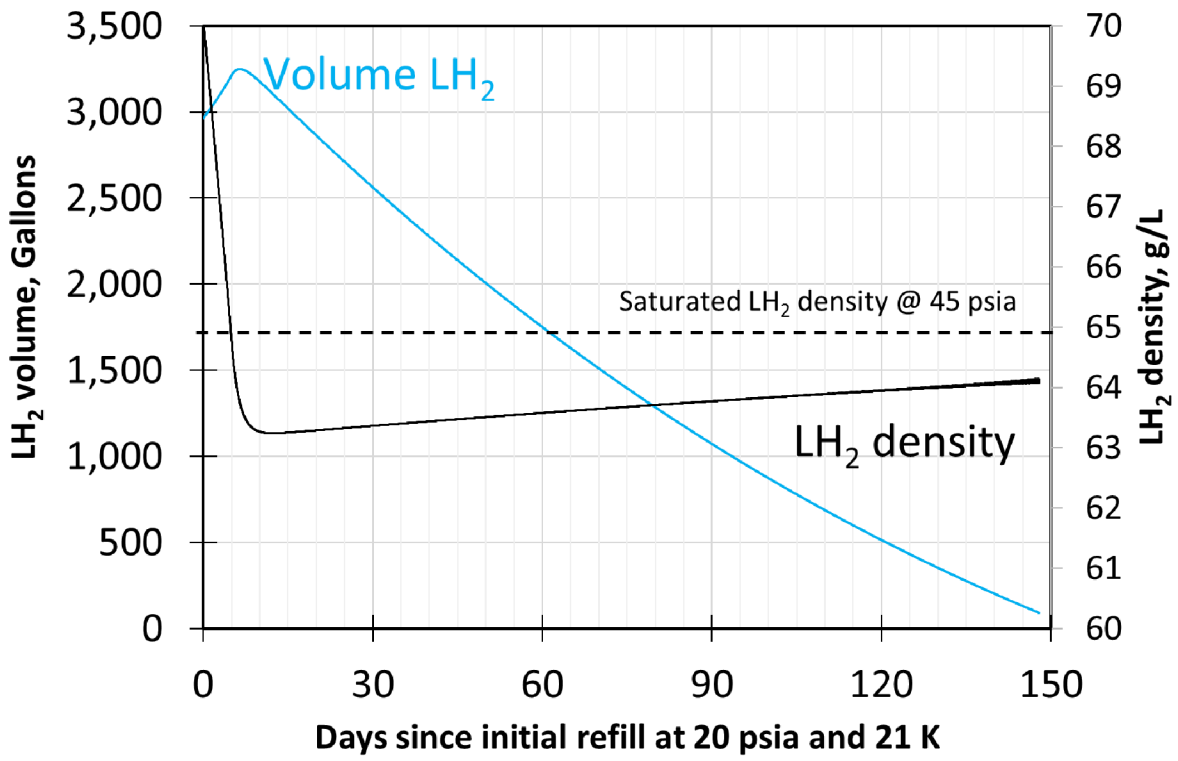

Figure 11: Variations of LH_2 volume (left axis) and density (right axis) for a 3,300 gallon Dewar with a 45 psia set pressure relief and exposed to the heat transfer with the environment shown in **Figure 8** ("Summer 2015"). The tank is initially filled with 3,000 gallons LH_2 at 20 psia and 21 K (uniform temperature distribution). The saturated liquid density at 45 psia is also shown for reference (64.92 g/L). Results computed with MATLAB code.

3.1.2. Boil-off from the liquid trailer (# 7016) under heat transfer with environment only (static)

The insulation performance of a LH_2 trailer is usually reported as the time between 2 different pressures at a certain capacity of H_2. **Figure 12** below shows a picture of this information as printed on the right side of liquid trailer #7016. Filling density numbers refer to the equivalent mass of product should the trailer be filled with water. For example, a 6% filling density correspond to 6% of 141,610 lbs. (water at 8.32828 lbs./gallon density per CFR title 49 173.318(f)(2) [20], in 17,000 gallon trailer) thus 8,496 lbs. or 3,853 kg of H_2.

According to DOT regulations (CFR title 49, subtitle B, Chapter I, Subchapter C) 173.318(g)(2)(ii) [20]), the marked rated holding time is equal to the One Way Travel Time (OWTT) plus 48 hours. For example, at 6.0% filling density, it is expected that the vapor pressure in the trailer raises from 30 to 50 psig in 110+48=158 hours. Using different constant heat transfer to simulate the pressures rise in the trailer, it was found that under those conditions an expected value for the heat transfer from the environment to the trailer was 270 Watts. This value was used for the rest of the study.

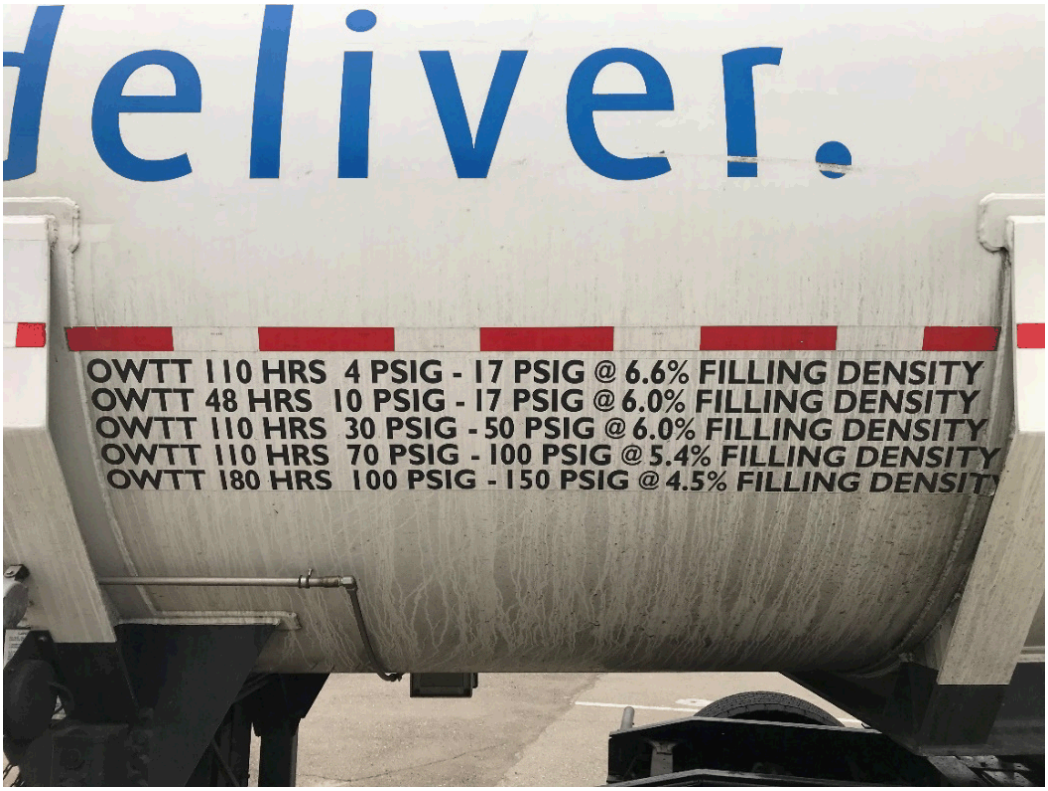

Figure 12: One Way Travel Time (OWTT) marking on the right side of trailer #7016, as required by the Code of Federal Regulations, title 49 173.318(g) [20].

3.2. Transfer from the terminal to the liquid trailer

As mentioned in **Table 1**, the trailer is typically to vented down to 4 to 8 psig (or 18.7 to 22.7 psia) before being refilled at the terminal. Depending of the pressure and the inventory in the trailer before venting, various amounts of H_2 may be vented. The vented fuel, however, is not considered as wasted since it is recirculated back to the liquefaction plant. The same holds true for the transfer losses: vented H_2 during transfer goes back to the plant. **Figure 13** and **Figure 14** show the variation of masses (liquid, vapor, and vented, bottom and top), temperatures and vapor pressure in a 17,000 gallon LH_2 trailer initially with 200 kg H_2 at 30 psia, that is first vented to 20 psia then filled starting at t=1hour until maximum capacity (here, 8,400 lbs. or 3,810 kg). There is initially 35 kg of liquid and 165 kg of vapor. About 40 kg of vapor is first vented to bring the pressure from 30 to 20 psia. A small amount of vapor is condensed (~200 grams) into liquid during that initial vent. The liquid fill then starts at t=1 hour and the liquid temperature quickly drops. When the pressure in the LH_2 trailer hits 22 psia, some vapor is vented until the pressure goes below 21.5 psia, then the relief valve is closed again until the next cycle.

A total of 3,810-125-35=3,650 kg of H_2 has been transferred from the liquefaction plant to the LH_2 trailer, and 40+80 =120 kg has been vented, i.e. 3.3 % of the of the transferred H_2 has been recycled back to the liquefaction plant.

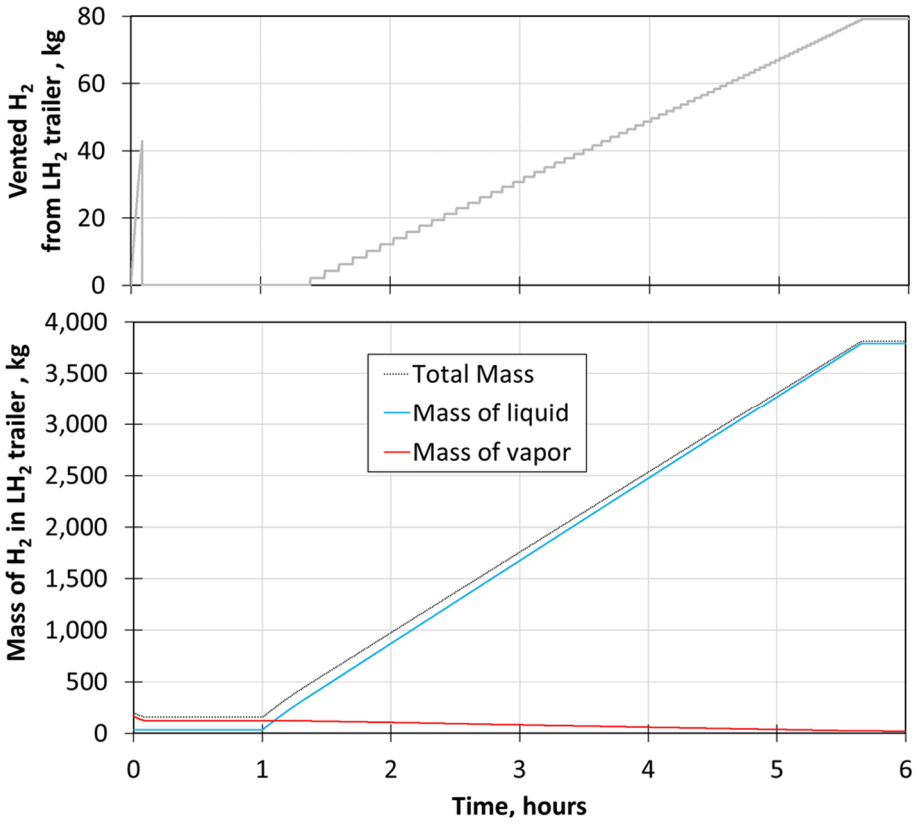

Figure 13: Mass of H_2 (bottom) and vented H_2 (top) for a 17,000 gallon LH_2 trailer initially with 200 kg H_2 at 30 psia, 20 K liquid temperature, 23 K vapor temperature and 20.5 K wall temperature. The trailer is first vented to 20 psia then fill starts at t=1hour, until the maximum capacity is reached (here, 8,400 lbs. or 3,810 kg). The vent pressure is set at 22 psia, and the heat transfer from the environment is 270 Watts. Corresponding temperatures and vapor pressure are shown in **Figure 14**. Results computed with MATLAB code.

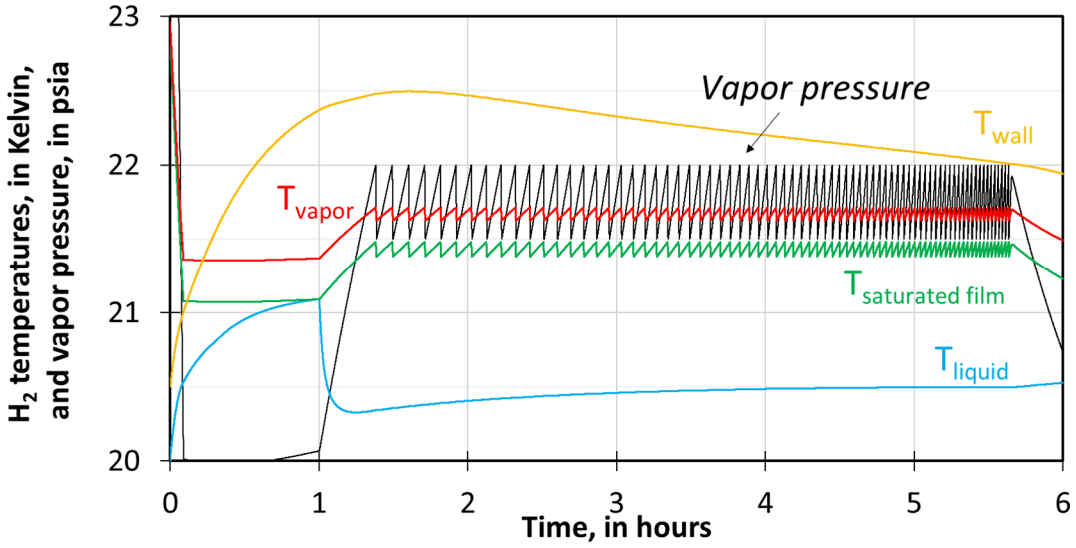

Figure 14: Temperatures (liquid, saturated film, vapor and wall) and vapor pressure in the 17,000 gallon LH_2 trailer initially with 200 kg H_2 at 30 psia, 20 K liquid temperature, 23 K vapor temperature and 20.5 K wall temperature. The trailer is first vented to 20 psia then fill starts at t=1hour, until the maximum capacity is reached (here, 8400 lbs. or 3810 kg). The vent pressure is set at 22 psia, and the heat transfer from the environment is 270 Watts. Results computed with MATLAB code.

3.3. Transfer from the liquid trailer to the station

As said earlier, the H_2 in the trailer needs to be pressurized using the onboard vaporizer to a vapor pressure larger than the pressure in the station storage system to be able to transfer the fluid. During the transfer, the vented H_2 from the stationary Dewar (receiving vessel) is typically not recovered, and neither is the H_2 vented from the trailer depressurization: H_2 is considered as pure loss under those 2 mechanisms.

Figure 15 and **Figure 16** show the simulated temperatures, vapor pressure and mass variations in the feeding vessel (top: 17,000 gallon trailer) and the receiving vessel (bottom: 3,300 gallon vertical Dewar). The delivery vapor pressure in the trailer is 60 psia, while the maximum pressure in the receiving vessel is 45 psia (setpoint for the pressure relief device). The fill takes less than 45 minutes to complete under those assumptions. During that time, 25 kg of H_2 boils away from the receiving vessel; and more than 100 kg is vented from the trailer when it is depressurized from 60 to 20 psia. We can also notice the initial increase of vapor pressure and temperature in the trailer, which corresponds to the initial pressurization (using trailer vaporizer) used to create a pressure difference between the 2 vessels.

Figure 17 the variations of the terms contributing to the energy balance of the vapor phase (top) and the liquid phase (bottom) of the receiving vessel (see also Equations 5 and 6). The term "Q_V" and "Q_L", black lines, are the summation of all other terms. We can see that the major contributor to the positive energy flow going into the vapor phase is the "-pdV" term (up to 1,300 Watts), that corresponds to compression force onto the vapor space resulting from the liquid phase's volume growing as the fill goes on. This incoming heat results in transfer losses from the receiving vessel (~25 kg). The governing mechanisms are quite different in the liquid phase (bottom figure) where the internal energy is mainly controlled by the energy of the incoming fluid (blue line); between 16 and 20 kW.

Figure 18 shows the influence of initial pressure in the receiving vessel on the vented H_2 from transfer losses. 4 different scenarios are represented (varying maximum pressure in the receiving vessel between 60 and 120 psia, 1% and 75% initially full vessel) and it appears that maximum pressure in the receiving vessel (or setpoint for the Pressure Relief Device or pressure regulator) does not have a strong influence on the magnitude of the transfer losses – see colored symbols. Alternatively, the initial pressure will strongly affect the transfer losses, from 2% at atmospheric pressure to almost 17% near 115 psia… Note that those simulations were performed assuming bottom fill injection method, and a discussion on the injection method will be provided later.

At last, the venting losses from the trailer potentially represents a very important source of boil-off losses, as illustrated in **Figure 19** where various simulations of trailer depressurization from initial H_2 masses between 3,800 and 200 kg, and initial pressures between 40 and 120 psia can be seen. The losses are of course an increasing function of the initial pressure. Additionally, those venting losses become more and more important as the initial mass of H_2 in the trailer decreases since more and more vapor is present. Those venting losses are the results of very extreme scenarios, and the rationale for those losses will be reviewed later in this document.

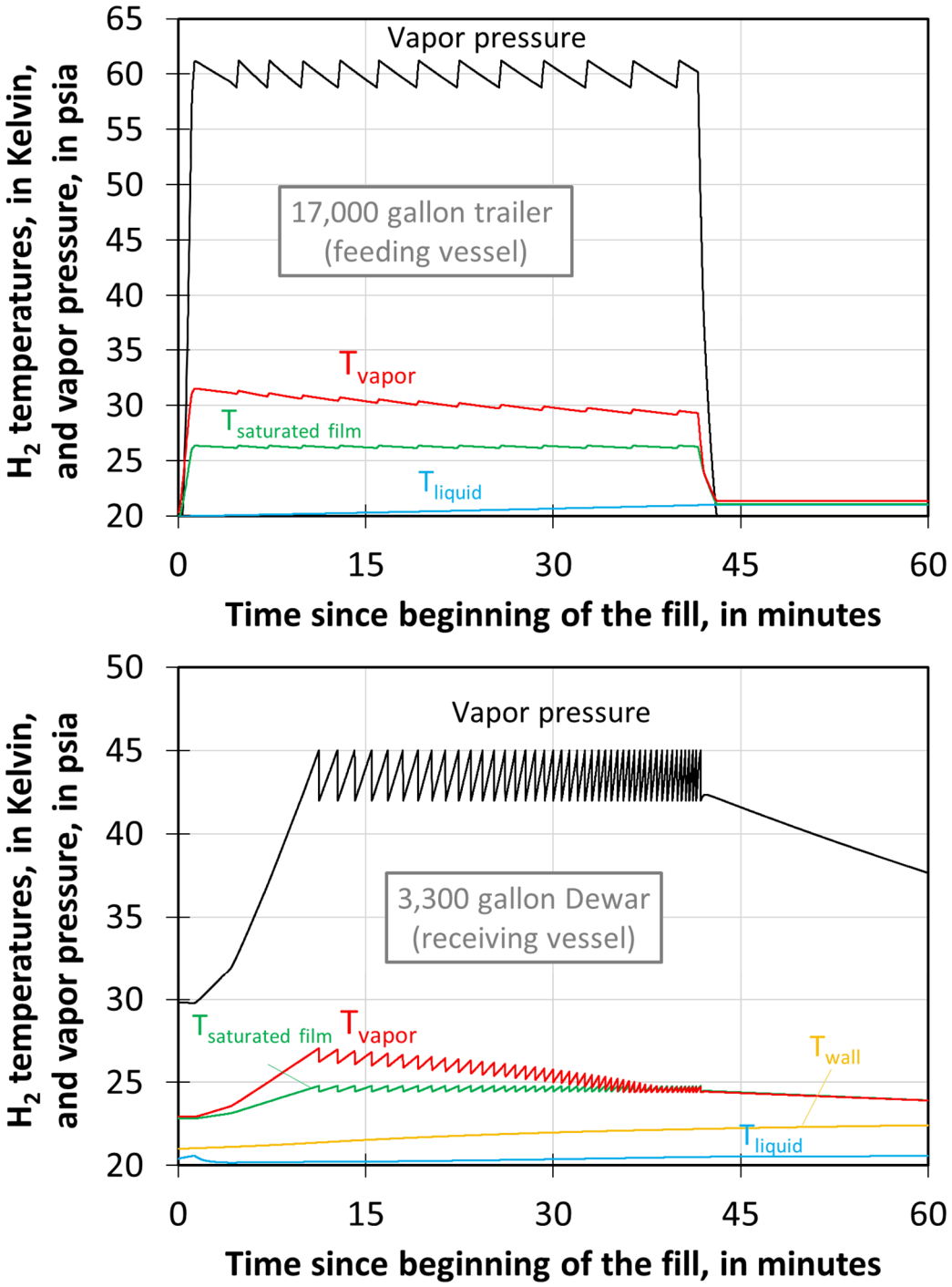

Figure 15: Temperatures (liquid, saturated film, vapor and wall) and vapor pressure in the trailer (top) and Dewar (bottom) during the fill. Results computed with MATLAB code.

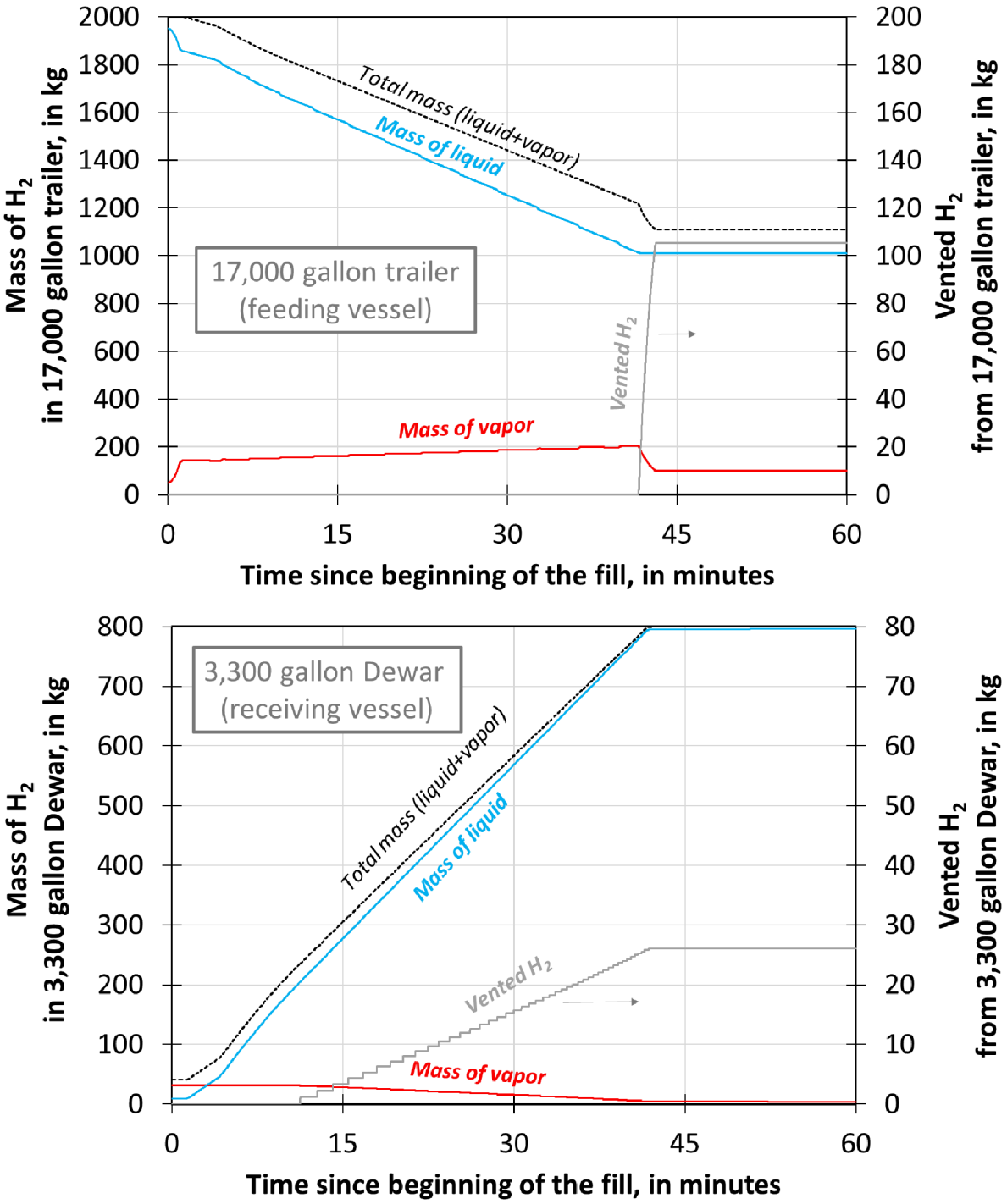

Figure 16: Mass of H_2 in vessel (liquid and vapor, left axis) and vented H_2 (right axis) in the trailer (top) and Dewar (bottom) during the fill. Results computed with MATLAB code.

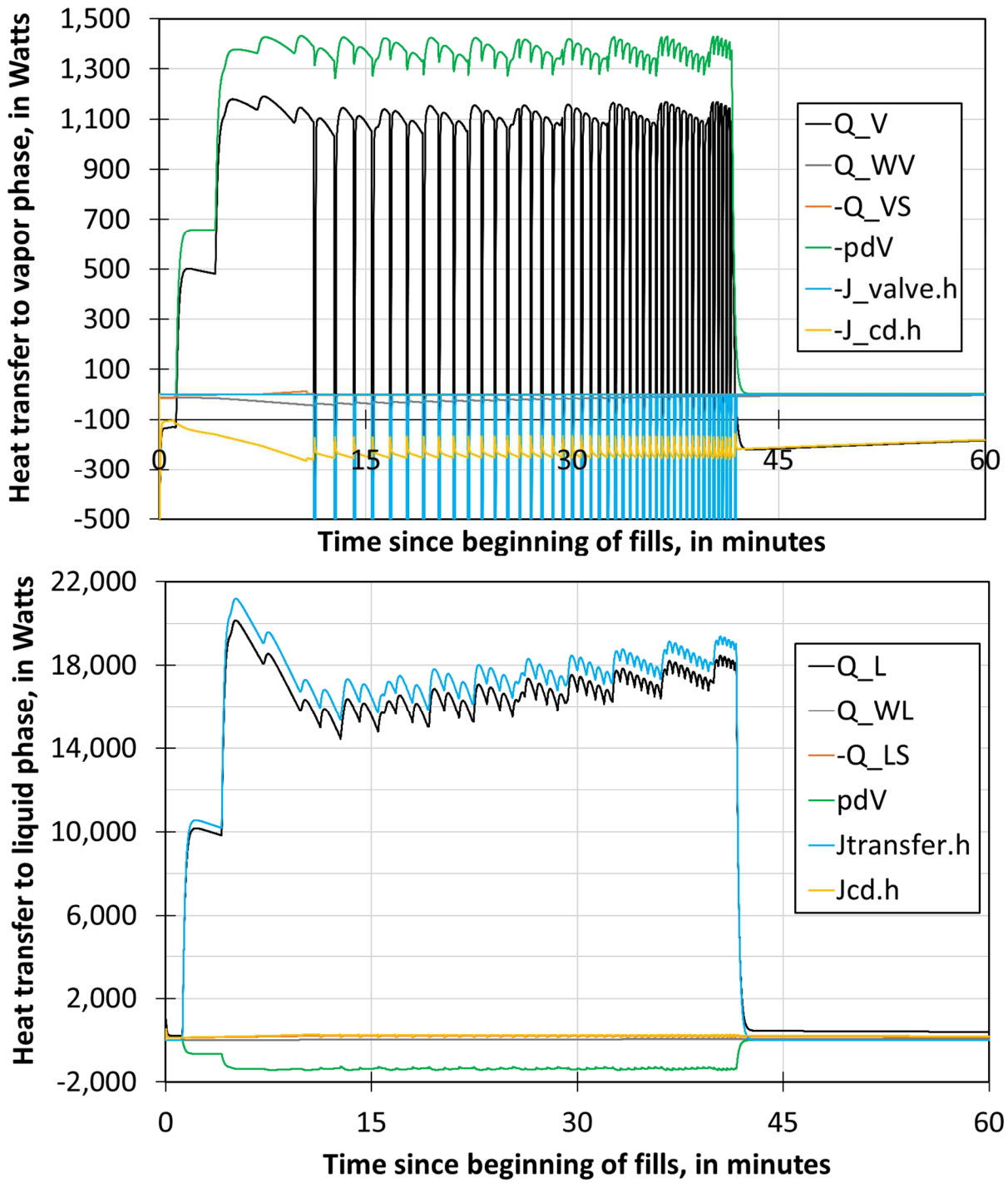

Figure 17: Heat transfer into the vapor phase (top) and the liquid phase (bottom) of the 3,300 gallon receiving vessel during fill from a 17,000 gallon trailer using bottom fill. The terms correspond to equations (5) and (6). Results computed with MATLAB code.

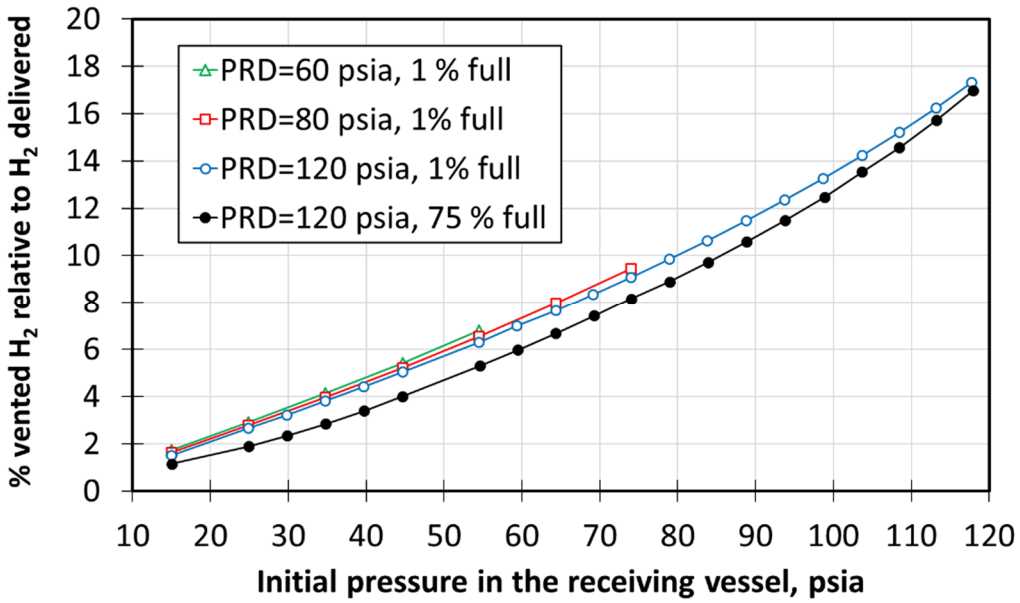

Figure 18: %vented H_2 from the receiving vessel (here: 3,300 gallon vertical Dewar) as a function of the initial pressure in the vessel, from a trailer pressurized to 140 psia and using bottom fill. 4 different simulations are represented: 3 runs were started at 1% inventory in the receiving vessel with 3 different maximum pressure (Pressure Relief Device = 60, 80 and 120 psia), while the 4th run was started with a 75% inventory and a maximum pressure of 120 psia. Results computed with MATLAB code.

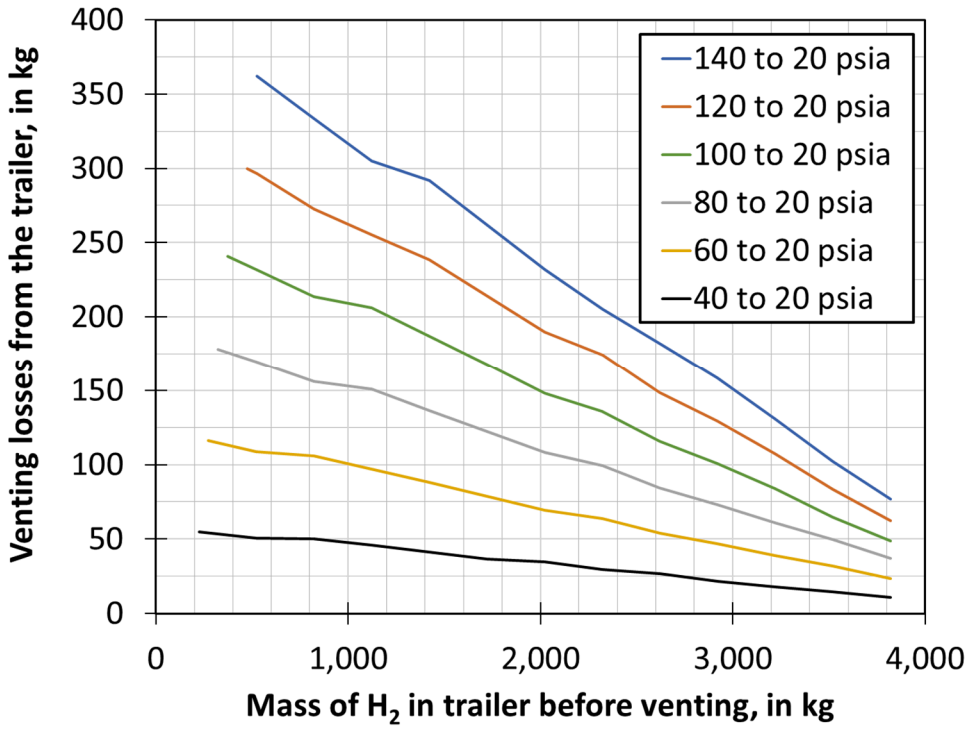

Figure 19: Simulated venting losses from the trailer as a function of initial mass of H_2 in the trailer for different venting pressures (40 to 140 psia), for an ending pressure to 20 psia. Results computed with MATLAB code.

4. Solutions to reduce/eliminate losses during LH_2 transfer at the hydrogen refueling station

From the results presented in the previous section, it appears that most of the LH_2 losses occur at the refueling station, when transferring and using the fuel. Addressing boil-off issues should first consider modifications to existing practices and operation to evaluate the opportunities for boil-off reduction with no/minimum additional cost, and only then investigate implementing solutions to capture boil-off losses that remain (next section). Those options are reviewed here.

4.1. Trailer depressurization

Trailer depressurization losses take place when the LH_2 trailer needs to reduce its pressure. LH_2 trailers usually deliver hydrogen using pressure difference: H_2 flows from the trailer to the receiving vessel as long as the total pressure difference is positive. At the end of the delivery, the vapor pressure in the LH_2 trailer is high and *may* need to be reduced before the LH_2 trailer can be driven on public highways, per CFR/DOT regulations, title 49 §177.840(i).

The Code of Federal Regulations written by Pipeline and Hazardous Materials Safety Administration at the Department of Transportation (Title 49, Volume 2, Subtitle B, Chapter I, Subchapter A, part 177) stipulates for class 2 (gases) materials that [20] :

> §*177.840(i)* No person may transport a Division 2.1 (flammable gas) material that is a cryogenic liquid in a cargo tank motor vehicle unless the pressure of the lading is equal to or less than that used to determine the marked rated holding time (MRHT) and the one-way travel time (OWTT), marked on the cargo tank in conformance with §173.318(g) of this subchapter, is equal to or greater than the elapsed time between the start and termination of travel. This prohibition does not apply if, prior to expiration of the OWTT, the cargo tank is brought to full equilibration as specified in paragraph (j) of this section.

Paragraph 177.840(j) mentioned in the above is reported below:

> §177.840(j) Full equilibration of a cargo tank transporting a Division 2.1 (flammable gas) material that is a cryogenic liquid may only be done at a facility that loads or unloads a Division 2.1 (flammable gas) material that is a cryogenic liquid and must be performed and verified as follows:
>
> (1) The temperature and pressure of the liquid must be reduced by a manually controlled release of vapor; and
>
> (2) The pressure in the cargo tank must be measured at least ten minutes after the manual release is terminated.

Paragraph 173.318(g) mentioned in the above is reported below:

> §173.318(g) *One-way travel time; marking.* The jacket of a cargo tank to be used to transport a flammable cryogenic liquid must be marked on its right side near the front, in letters and numbers at least two inches high, "One-Way-Travel-Time __ hrs.", with the blank filled in with a number indicating the one-way travel time (OWTT), in hours, of the cargo tank for the flammable cryogenic liquid to be transported. A cargo tank that is partially unloaded at one or more locations must have additional marking "One-Way-Travel-Time __ hrs. __ psig to __ psig at __ percent filling density," with the second blank filled in with the pressure existing after partial unloading and the third blank filled in with the set-to-discharge pressure of the control valve or pressure relief valve, and the fourth blank with the filling density following partial unloading. Multiple OWTT markings for different pressure levels are permitted. The abbreviation "OWTT" may be used in place of the words "One-way-travel-time" in the marking required by this paragraph.

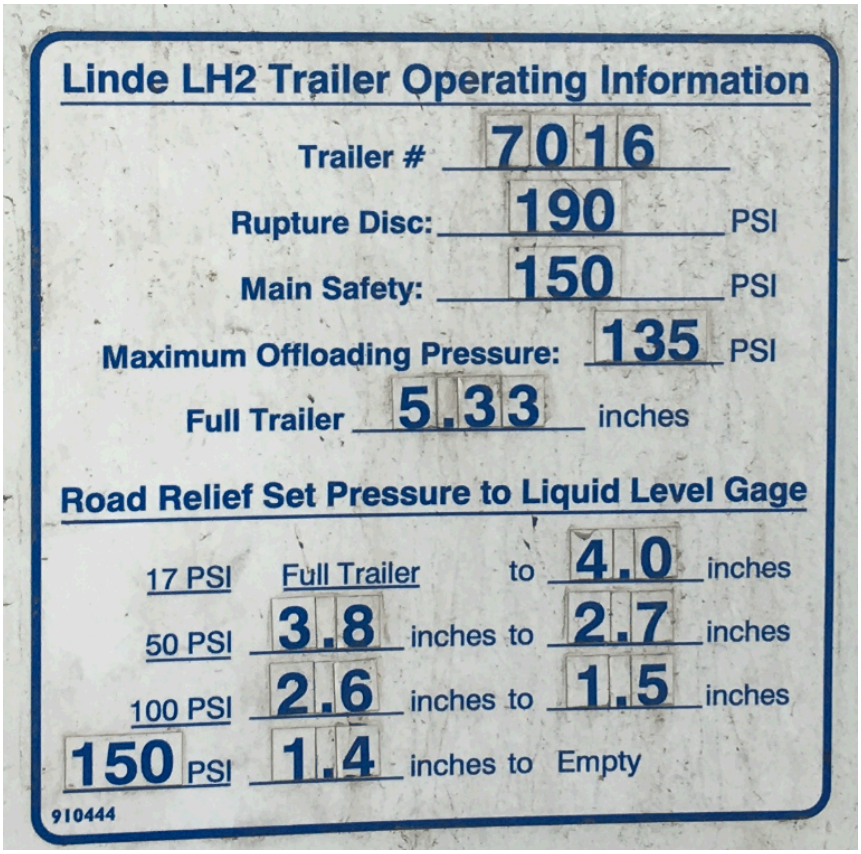

Figure 20: Required road relief set pressure (in psig) as a function of liquid level gage as required by the Code of Federal Regulations, title 49 173.318(f)(2), for trailer #7016

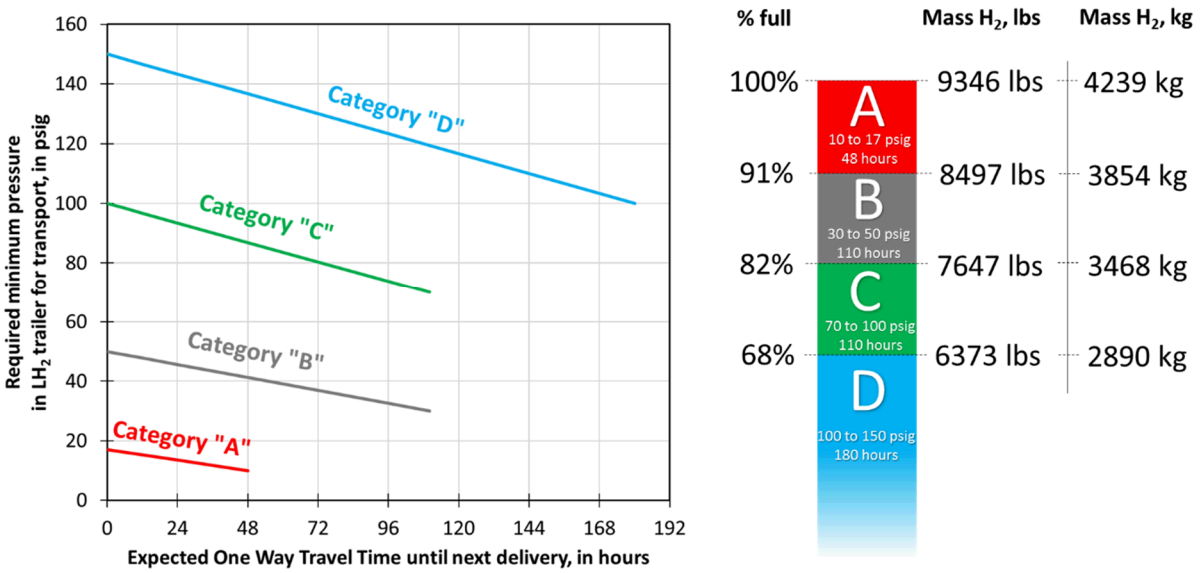

Figure 21: Interpretation of the Code of Federal Regulations concerning the requirements for the transport on public highway of cryogenic liquid division 2.1 flammable gas: 49 CFR 177.840(i) and 173.318(f)(2) [20], applied to LH_2 trailer #7016 – see corresponding markings on **Figure 12** and **Figure 20**. 49 CFR 177.840(i) requires a minimum pressure in the LH_2 trailer for transport, based on the quantity of H_2 in the trailer (categories A, B, C or D) and the expected travel time to next delivery. The figure on the left assumes a constant pressure rise.

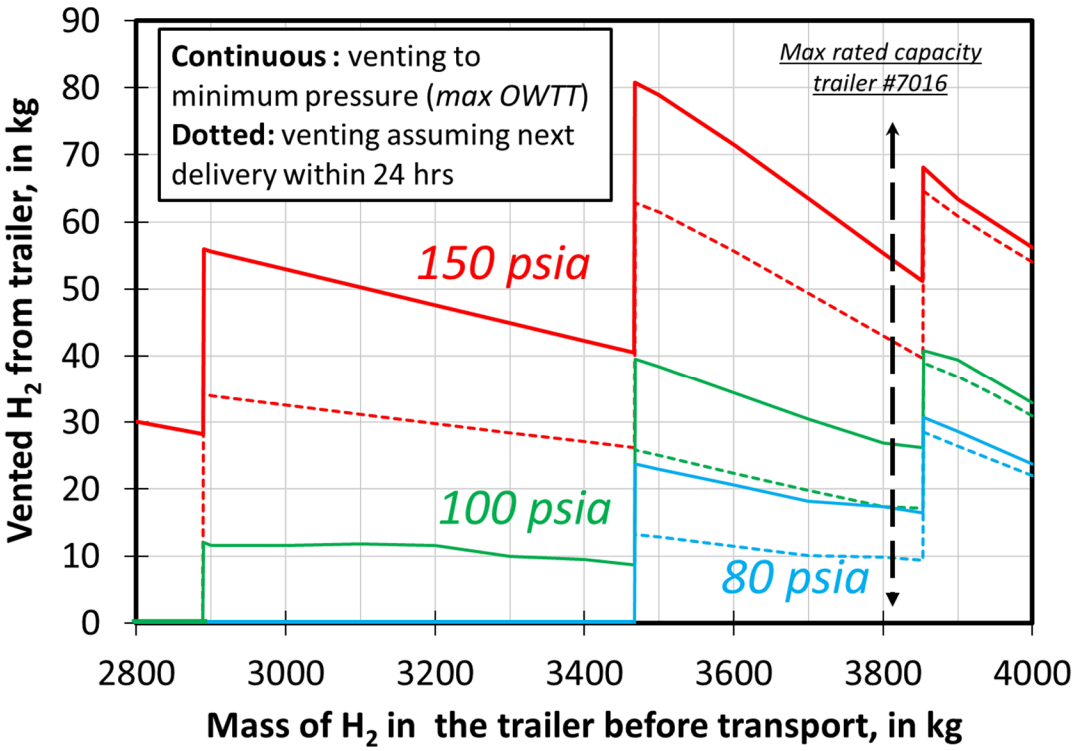

Figure 22: Simulated vented H_2 from trailer before transport, per DOT regulation (49 CFR 177.840(i)). The results are shown as a function of the mass of H_2 in the trailer before transport for the range 2,800-4,000 kg, for three initial vapor pressures (150, 100 and 80 psia), and 2 expected One-Way Travel Time scenarios: maximum OWTT (continuous lines), and 24 hours (dashed lines).

The amount of vented H_2 from the trailer necessary to comply with the CFR/DOT regulation is thus a function of the mass of H_2 in the trailer before transport, the vapor pressure, and the expected travel time until the next delivery. **Figure 22** shows the estimated amount of vented H_2 following CFR/DOT regulations as computed by our simulation code. The results are shown as a function of the mass of H_2 in the trailer before transport for the range 2,800-4,000 kg, for three initial vapor pressures (150, 100 and 80 psia), and two expected One-Way Travel Time scenarios: maximum OWTT (continuous lines), and 24 hours (dashed lines). The maximum rated capacity of trailer #7016 (8400 lbs., or 3,810 kg) is reported for reference, while its maximum offloading pressure is 150 psia (135 psig, see **Figure 20**). For initial vapor pressures of 100 and 80 psia in the trailer, no venting is necessary if the quantity of H_2 in the trailer before transport is below 2,890 and 3,468 kg, respectively. If another delivery is expected within the next 24 hours, amounts below 3,468 kg do not need to be vented if the vapor pressure is 100 psia or below, and the maximum vented H_2 for any quantities of H_2 in the trailer at 100 psia decreases from 40 to 25 kg. Those values decrease from 24 to 12 kg for an 80 psia initial vapor pressure.

A delivery vapor pressure of 80 psia (or lower…) in the trailer is typical of refueling stations using a cryo-pump, whose Dewar's set pressure relief device is 45 psia (30 psig). Assuming a max capacity of 3,810 kg (e.g. trailer #7016), no venting of H_2 is required per CFR/DOT regulation after the first delivery if more than 3,810-3,468=342 kg is delivered, which is expected as many stations are rated for at least 400 kg/day. All subsequent deliveries at similar pressures are evidently not required to vent any H_2 per CFR/DOT regulation.

For a compressor-based station, the vapor pressure in the Dewar is the range of the allowable suction pressure for the compressor. Assuming a 75 to 105 psia range (60 to 90 psig), pressures as high as 125 psia could be needed in the LH_2 trailer… In order to avoid subsequent venting losses from the trailer, the stationary storage may be vented down to ~80 psia, thus 100 psia in the LH_2 trailer. This makes sense from the losses perspective as long as the stationary storage does not vent more than what would be wasted from the trailer. From an operation perspective, it is also faster to vent the stationary storage than pressurizing the trailer. Assuming 100 psia, a maximum amount of 40 kg would need to be vented if less than 342 kg is delivered (less likely), and a maximum of 12 kg would need be vented if less than 3810-2890=920 kg is delivered during the first fill. The amount vented during the subsequent fills is of course scenario dependent. Please note that small quantities of H_2 (estimated <1 kg) are vented to pre-cool the pipe and during disconnection. Those quantities are not well quantified yet.

4.2. Transfer losses from the receiving vessel

Boil-off losses from the receiving vessel during the LH_2 transfer is one of the most important sources of H_2 losses along the LH_2 pathway. This losses phenomenon is due to the vapor being compressed (= pdV work) by the liquid phase as the receiving vessel is filled with liquid.

This issue and how to mitigate it is very important for the aerospace industry, where conventional fill techniques on the ground cannot really be applied in micro-gravity and propellant is at a premium cost [21]. As such, a few studies can be found in the literature concerning the concept of No-Vent Fill (NVF), summarized below.

Researchers at the NASA Lewis Research Center (Cleveland, OH) have carried out systematic analysis of no-vent fills of liquid hydrogen tanks of different internal volumes: 34 Liters [22], 142 Liters [23], 2 m^3 [24], and 4.96 m^3 [25]. At least 4 different injection methods were tested: top spray, upward pipe discharge, bottom diffuser [22] , and spray bar [23]. Various spray nozzle designs were also looked at [25]. Among the many results, it was found that the final fill level (or state of charge) was directly proportional to the inlet liquid flow rate, and that the top spray was the most efficient no-vent fill method; due primarily to the condensation of the ullage vapor onto the incoming liquid droplets. This ullage condensation counteracts the tank pressure rise resulting from energy exchange between the fluid and the warmer tank walls [22]. This effect can be shown on **Figure 23**, where pressure rises are compared for 2 different injection methods (top and bottom). A spray bar was shown to have a similar effect as the top spray [23] (see illustration on **Figure 24**).

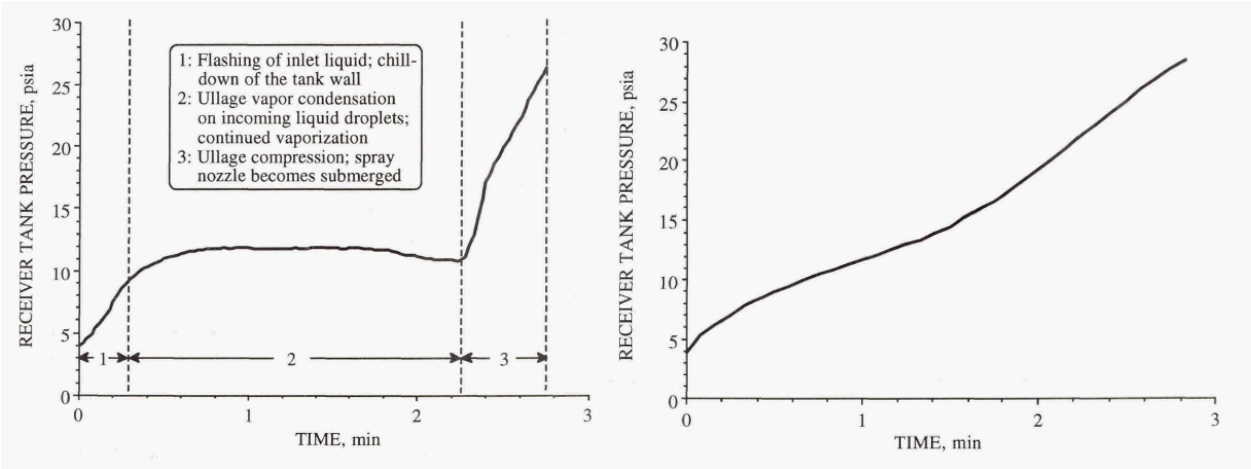

Figure 23: Comparison of pressure history between top spray (left) and bottom diffuse (right) injection techniques for a 34 Liter tank, from [22]

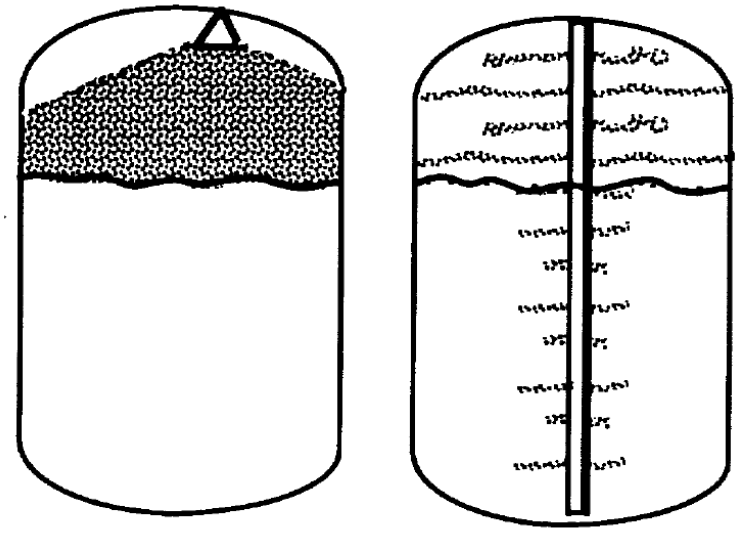

Figure 24: Spray nozzle (left) and spray bar (right) injection techniques, from [23]

In addition to the experimental investigation, analytical models were developed at the NASA Glenn Research Center, such as NVFILL ([25], [26]) that uses a correlation to calculation the convection coefficient between the spray droplets and the ullage and where the vapor and the liquid are not necessarily at equilibrium (similarly to the MATLAB code we used), or the Cryogenic System Analysis Model (CSAM) computer code [27]. Two more computer codes were developed: GDNVG (General Dynamics No-Vent Fill), by General Dynamics, and NVEQU (Non Vented EQUilibrium), by NASA Lewis Research Center. See more details in [21]. More recently, researchers from the NASA Kennedy Space Center demonstrated through the GODU-LH_2 project, concurrently with a Zero Boil-Off approach using cryo-refrigeration [28], that a no-vent fill of a 33,000 gallon LH_2 vessel could be performed at all fill level using refrigeration [29], [30], [31].

Two more groups have made significant contributions to the understanding of No-Vent Fills in the recent years: the group of Sangkwon Jeong at the Korea Advanced Institute of Science and Technology (Daejon, South Korea) [32], [33], [34], and the group of Yanzhong Li and Lei Wang from the Xi'an Jiaotong University (Xi'an, China) and the State Key Laboratory of Technologies in Space Cryogenic Propellants (Beijing, China) [35], [36] [37].

From the results on No-Vent fill investigations for aerospace applications, performing top fill of the stationary storage during the transfer may be a worthwhile idea to limit the transfer losses. A top fill of our 3,300 gallon vessel was performed at our facility at Lawrence Livermore National Laboratory (Livermore, CA) on 02/20/2018, from a trailer maintained at 55 psig – see **Figure 25**. Vapor pressure (red line, left axis), and level (blue line, right axis) were recorded every minute, for a vessel initially at 32 psig with 1.5 inH_2O of LH_2. The boil-off from the main stack was also measured (every 5 seconds) during the fill. The only boil-off that could not be measured (boil-off via non-monitored stacks) were the initial cooling/purging of the line, and the boil-off when the tri-cock valve was opened. **Figure 25** shows that after an initial decrease (t=1 min), the vapor pressure then increases until it reaches a plateau (t=6 minutes) with a slight decrease, a behavior similar to what was observed in No-Vent fill experiments (see for example **Figure 23**) and corresponding to initial flashing of inlet liquid and ullage vapor condensation, respectively. The vapor pressure and boil-off flow follow similar variations during the fill, and a decrease is observed between t=21.5 min and t=24 min, when the tri-cock valve is opened to allow a more precise measurement of the liquid level near the top. During that time, some boil-off is not measured by the boil-off meter, estimated to amount to around 20 grams based on the boil-off trend before and after the tri-cock vale opening. Overall, less than 1 kg of H_2 is lost during the 532.5 kg LH_2 delivery, which is significantly less than the losses simulated with a bottom fill (see above). This result experimentally confirms the relevance of top fill to reduce transfer losses. It is also possible that lower losses may be achieved when varying the initial conditions in both the feeding and receiving vessel and optimizing the fill procedure.

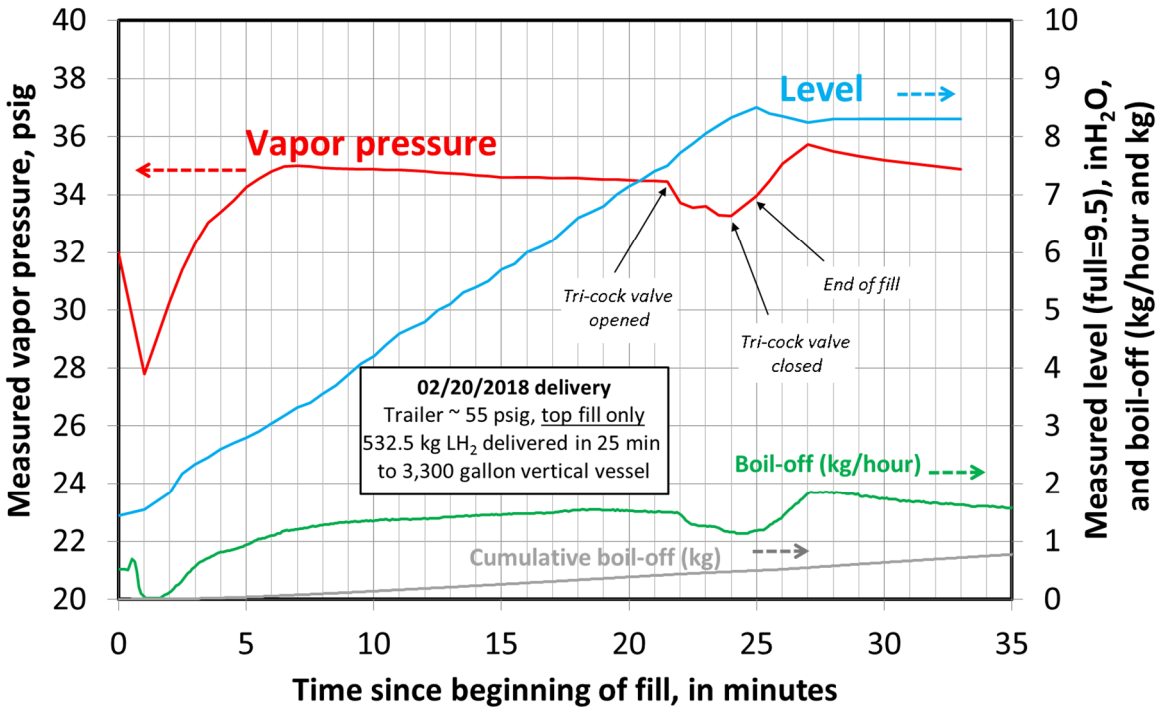

Figure 25: Pressure, level and boil-off variations measured during the top fill of a 3,300 gallon vessel at Lawrence Livermore Laboratory (Livermore, CA)

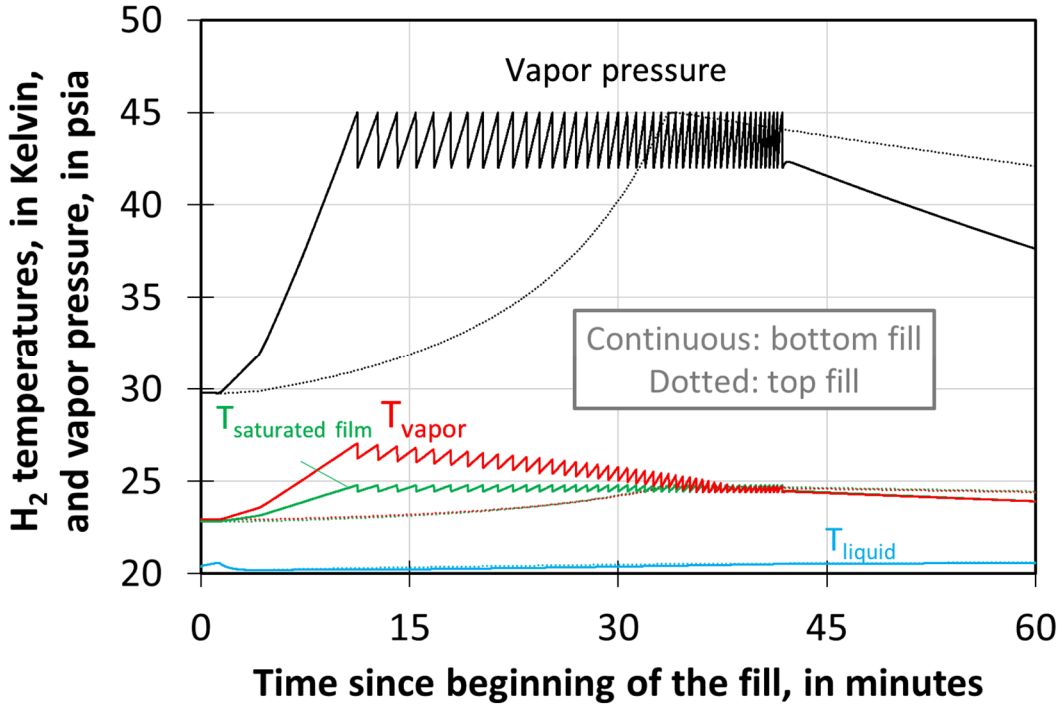

Figure 26: H_2 temperatures and vapor pressure variations for a bottom (continuous lines) and a 3.08% top fill (dotted lines), as computed by the MATLAB code.

Our MATLAB code does not have the capabilities to account for the various physical phenomena taking place with sprays (boiling heat transfer as a function of temperature, droplets/vapor interaction…) for top fills. In the future more detailed CFD based simulations could be used to more adequately represent and understand the underlying physics of No-Vent Fills and sprays, similarly to the work by Li and Wang ([35], [36], [37]), the thesis by Keefer [38] or Wang *et al* [39]. For this current work, we implemented a simple approach in the MATLAB code where only a fraction of the top filled LH_2 is evaporated, and the rest goes directly to the liquid phase as a liquid droplet – see section 2.2.3 of this document. **Figure 26** shows a comparison of a simulation of a bottom fill (continuous lines) vs a top fill (dotted lines), where 3.08% of the liquid is vaporized, corresponding to 1 kg of transfer losses. Again, this model is only a crude approximation of the physics taking place, and its sole purpose is to illustrate the effects of top fill on the thermodynamic state. For example, the vapor pressure variations are very different from the ones experimentally measured in **Figure 25**… The vapor and saturated film temperatures are colder for the top fill than for the bottom fill, which makes sense since the vapor pressure is lower during most of the fill.

4.3.Low pressure LH_2 transfer pump

An alternative strategy to avoid the need for trailer pressurization and provide very low temperature LH_2 which would ultimately reduce transfer losses would consist in using a low pressure LH_2 pump that could transfer LH_2 from a low pressure LH_2 trailer. Such a solution, however, may add heat to the LH_2 being transferred and ultimately reduce the transfer efficiency. A commercially available solution is detailed in **Table 2**, adding an estimated 700 Watts for a 1000 kg/hour flow rate. The LH_2 pump addition was simulated with the MATLAB code, where the transfer enthalpy term was modified to consider additional heating from the pump as a H_{pump}/q_{flow} term. **Figure 27** show the variations of temperatures in the LH_2 trailer and the receiving vessel using either pressure differential (dotted lines) or a transfer pump (continuous lines) to accomplish transfer. Temperatures are lower in the LH_2 trailer when using the transfer pump since the vapor pressure and thus the saturated film temperature are kept at a lower value. This effect somewhat reduces the impact of the extra heating of the pump since the H_2 entering the pump has then a lower enthalpy. As result, the effect of the extra heating on the LH_2 internal energy and temperature in the receiving vessel (**Figure 28**) is also reduced: a maximum temperature difference of 0.15 Kelvin is observed midpoint into the transfer, and it is only 0.06 K at the end of the transfer. Final conditions in the receiving vessel using either transfer method are summarized in **Table 3**. From those results and under those conditions, it is concluded that the effect of extra heating from a low-pressure transfer pump is negligible. Therefore, such a solution should be implemented provided it makes sense from an economic standpoint.

Table 2: Performances of a low pressure LH_2 pump with a 35 psia inlet pressure and a 65 psia outlet pressure, with a 1,000 kg/hour flow rate, as quoted by Barber-Nichols on 12/5/2017.

Operation Condition	Value
Operating Speed	17,000 RPM
Estimated Pump Efficiency	55%
Estimated Pump Shaft Power	1495 Watts
Estimated Electrical Power	1720 Watts
Estimated Conducted Heat Rate (when installed within a vacuum cold box)	30 Watts thermal
Estimated Heat Rate due to Pump Inefficiency	673 Watts thermal

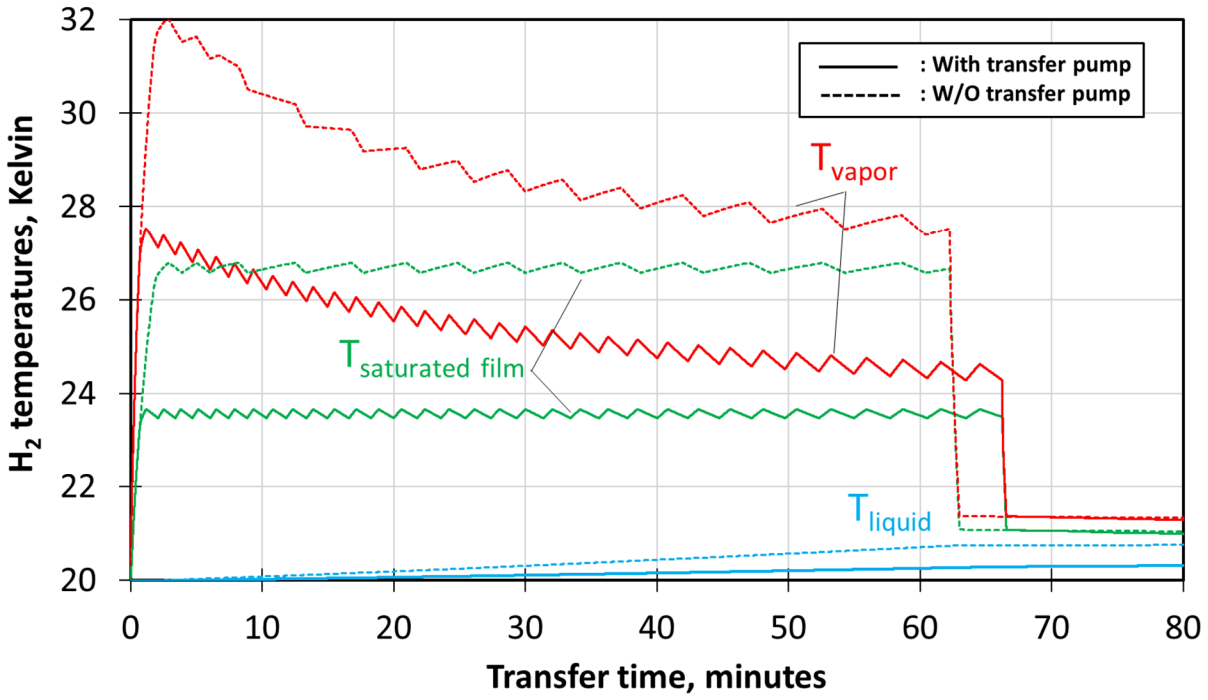

Figure 27: H_2 temperatures (liquid, saturated film, vapor) in the LH_2 trailer during transfer, using either pressure differential (65 psia to fill a 45 psia vessel, dotted lines) or a transfer pump (35 psia to fill a 45 psia vessel, continuous lines). Results computed using the MATLAB code.

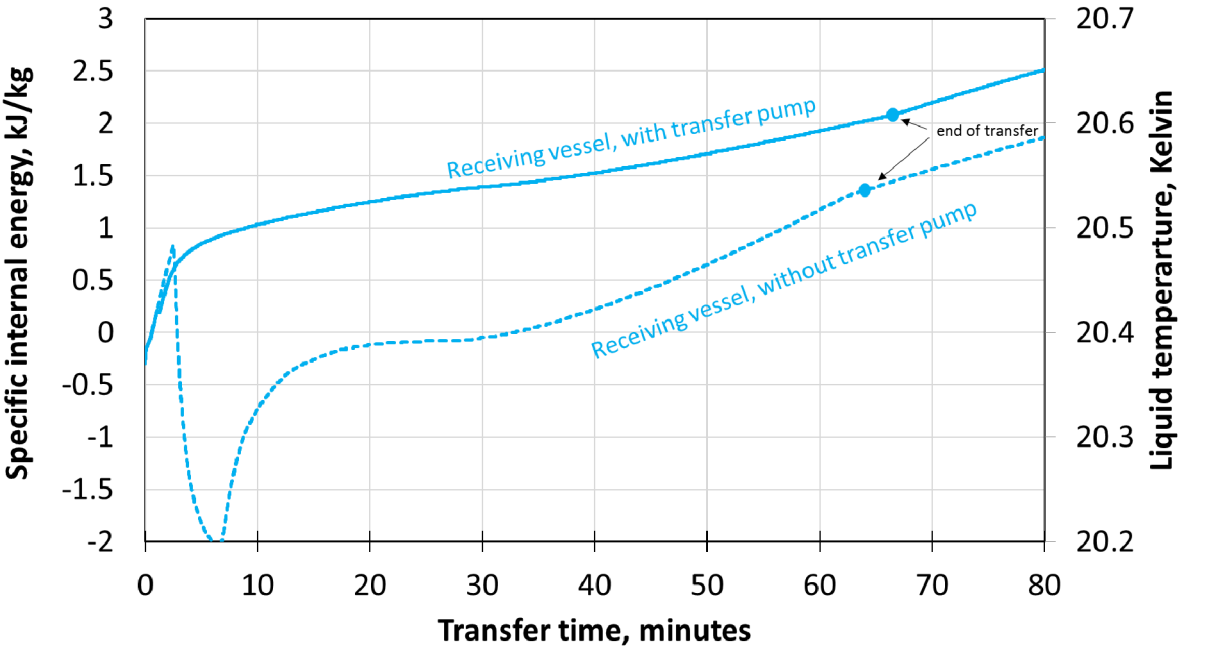

Figure 28: Variations of specific internal energy and temperature in the liquid phase of the receiving vessel (3,300 gallon Dewar with a 45 psia pressure relief device) during the transfer from the LH_2 trailer, using either pressure differential (dotted line) or a transfer pump (continuous line). Specific internal energies and temperatures are not strictly identical, but their values are close enough to be represented as such. Results computed using the MATLAB code.

Table 3: Final conditions in the 3,300 gallon receiving Dewar (set pressure: 45 psia), initially with 30.6 kg of H_2 at 20.1 K, using either the pressure differential or the transfer pump method. Results computed using the MATLAB code.

	Pressure differential transfer method (65 psia)	**Transfer pump (35 psia)**
Mass of liquid, kg	794.1	793.1
Mass of vapor, kg	4.1	4.1
Total mass, kg	798.2	797.2
Transfer losses, kg	16.1	16.1
Liquid temperature, K	20.5	20.6
Saturated film temperature, K	24.7	24.7
Vapor Temperature, K	26	26

5. Boil-off budget up to dispensing, after boil-off reduction

Assuming the techniques described in the previous section have been implemented, especially top fill and no venting from the trailer per CFR/DOT, it is now possible to quantify the *improved* amount of boil-off losses expected along the LH_2 pathway, for a stationary LH_2 storage operating at reasonably low pressure (45 psia or so) and connected to a LH_2 pump.

As mentioned earlier, it is first assumed that no boil-off loss occurs at the liquefaction plant (including during LH_2 trailer refill), as most of it is recycled at the plant. Secondly, the travel from the liquefaction plant to the first delivery is considered fast enough (less than 48 hours) so that no H_2 is vented from the LH_2 trailer while on the road. Thirdly, it is assumed that no venting from the LH_2 trailer at the station is necessary, per CFR/DOT. This assumption appears realistic as it requires, at the minimum, the following: less than 24 hours between first two deliveries, more than 350 kg dispensed during the first delivery, and maximum pressures less than 80 psia.

For this work, the boil-off measured from a 875 bar LH_2 pump manufactured by Linde (and located on LLNL campus) is used as benchmark. Three different boil-off mechanisms from the pump are identified. At first, the secondary vessel in which the pump is submerged needs to be cooled down and filled with LH_2 (up to ~ 90%). **Figure 29** shows the variations of pump temperature (blue line), pressure (gray line) and level (green line), as well as instant and cumulative boil-off (black lines, continuous and dotted) from the entire station (pump vessel + stationary 3,300 gallon vessel) as a function of time of the day. A pump vessel initially empty and at ambient temperature will boil away around 5 kg of H_2 until it is full (12:30 PM to around 2:30 PM).

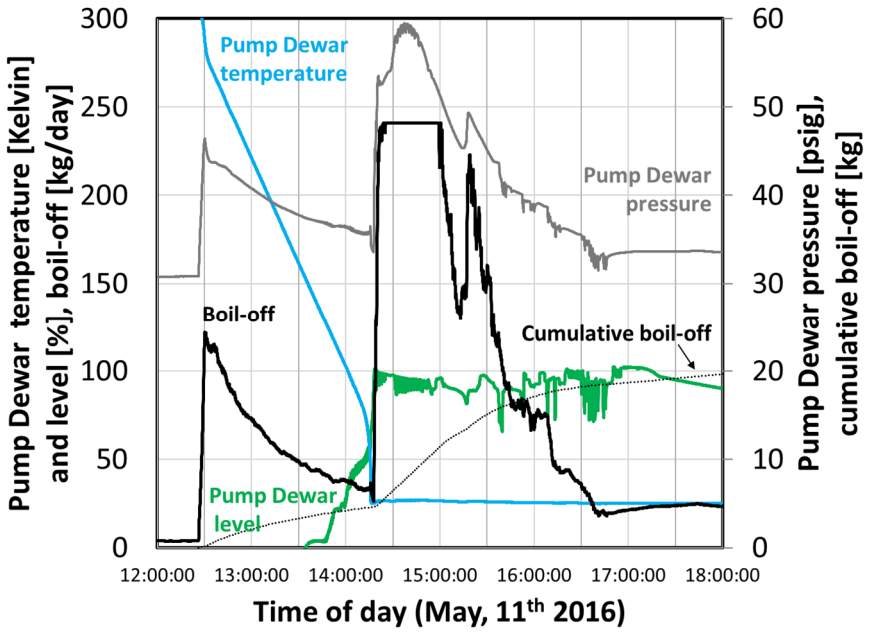

Figure 29: Pump Dewar temperature (blue), level (green) and pressure (gray, right scale), as well as boil-off (instantaneous: black, left scale; cumulative: dotted, right scale) during pump cool-down on May 11, 2016. The pump was run for system testing only, not for vessel cycling.

Under typical station utilization, however, the pump vessel would not be cooled down from ambient temperature but would rather see temperature cycles from lower temperatures, based on the frequency of utilization. **Figure 30** illustrates a more realistic utilization where the pump is used until about 6 PM then its vessel is being left warming up until the next day around 8 AM. Over this period, the pump warms up from 25 to only 50 K – see blue line. Then, when the pump is being cooled again, only 1 kg of H_2 is boiled away to reach a 100% fill level.

Figure 30 also shows a second boil-off mechanism, which is pump warm-up, or idling, when the pump is not being used and is left warming-up, here between 6 PM and 8 AM the next day. Over that timeframe, about 8 kg of H_2 is boiled away – see black dotted line, at a rate of ~0.5 kg/hr.

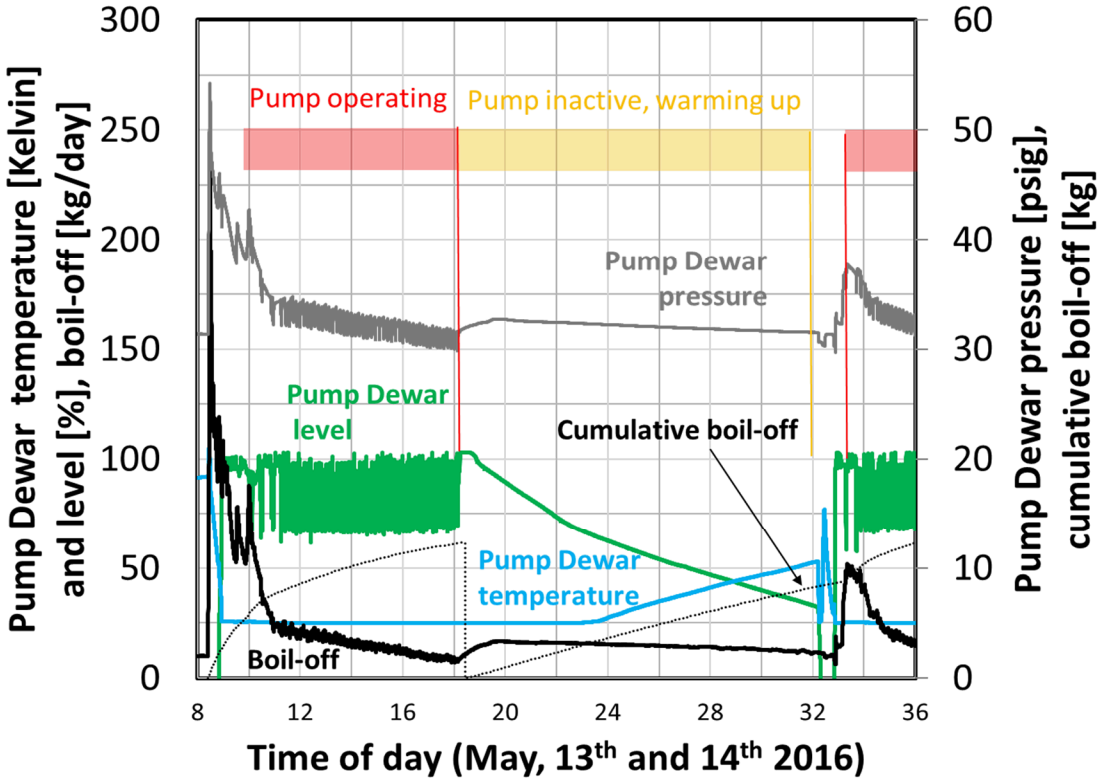

Figure 30: Pump Dewar temperature (blue, left scale), level (green, left scale) and pressure (gray, right scale), as well as boil-off (instantaneous: black, left scale; cumulative: dotted, right scale) on May 13-14, 2016.

The third boil-off mechanism due to the pump is attributed to due to actual pump utilization, when the pump pressurizes LH_2 up to 700 bar. It has been measured experimentally during pump operation the losses from the entire station (pump vessel + stationary 3,300 gallon vessel) could be as high at 3 kg/hour (during the first fills up to 700 bar), while zero boil-off situations have been observed, especially at lower fill pressure, and low level in the stationary storage. An average value of 0.6 kg/hour was measured over 7 different days of cycling and 456 fills to 700 bar – see **Figure 31**. Series of fills performed at lower pressures (300 to 350 bar) and not reported here have exhibited much lower boil-off during pump utilization, down to 0.01 kg/hr on average.

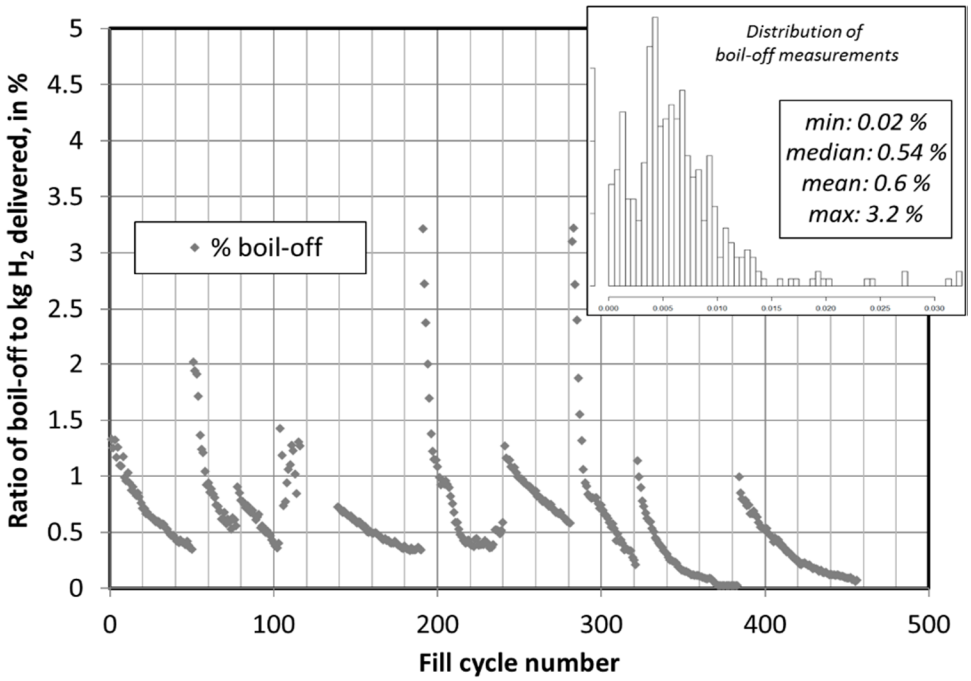

Figure 31: Measured percentage of boil-off for each cycle to 700 bar of the experimental vessel prototype. The inset on the top right of the figure shows the statistical distribution of the losses during the 456 cycles performed in May 2016, extending from 0.02 to 3.2%, with a mean value of 0.6%.

To summarize, it is considered that the boil-off losses along the entire LH_2 pathway, from liquefaction to dispensing, come from: 1) transfer losses from the receiving stationary vessel at the LH_2 station, 2) pre-cooling of the LH_2 pump, 3) boil-off from LH_2 pump utilization, and 4) boil-off from LH_2 pump warm-up/idling. **Table 4** summarizes our estimates of magnitude of the boil-off losses for each mechanism, mostly based on measurement obtained at LLNL. The magnitude of boil-off losses at a hydrogen refueling station is thus a function of how often the receiving stationary vessel is refilled and how the LH_2 pump is used (how many hours per day).

We next assume the following: the receiving stationary vessel's capacity is twice the daily capacity of the station (i.e. refill every other day); the number of dispensers is a function of the peak demand at the station, i.e. 7.8% of the station capacity (see [40]); each FCEV needs about 8 minutes to fill 5 kg (including lingering) so that a dispenser can deliver up to only 7.5 vehicles per hour; each dispenser needs one LH_2 pump, whose flow rate is 100 kg/hour; if the station needs multiple dispensers, then all LH_2 pumps are connected to the same submerged vessel.

The expected boil-off losses for each dispenser/LH_2 pump is then estimated by simulating the duty cycle of each dispenser during each hour of the day, assuming the demand profile presented in [40].

Table 5 and **Table 6** show our estimate of how the boil-off losses would contribute to the total boil-off budget as a function of station size (ranging from 100 to 5,000 kg/day), for 700 bar and 350 bar direct fills, respectively. Station sizes that see a low utilization of the pump (see 7th column) are assumed to have a greater boil-off from pump utilization (see 8th column). As a result, only station size above ~2,000 kg/day would experience minimum boil-off losses from pump utilization. The last column of each table shows the losses as a fraction of each LH_2 delivery (in %), which could be seen as the extra cost the end-user would

pay on average due to boil-off losses. **Figure 32** shows the losses at the pump (% of LH_2 delivered) for different station sizes, and 2 dispensing pressures (350 and 700 bar). The losses are relatively large at station sizes less than 400 kg/day (5 to 15% of LH_2 delivered), which is due to the low/moderate utilization of the LH_2 pump. Above 2,000 kg/day, the boil-off losses become less than 2% for 700 bar refueling and less than 0.7% for 350 bar refueling. **Figure 33** illustrates the relative contribution of each boil-off mechanism and highlights the fact that the boil-off from the pump when being used and idling/warming up is dominant.

Table 4: Boil-off mechanisms and magnitudes, assuming 100 kg/hr LH_2 pump. Most of those data have been measured experimentally on LLNL facility, using a boil-off meter that measures losses from entire system (pump + stationary storage) thus includes environmental heat transfer. Connection losses are assumed negligible

Boil-off losses mechanism	Expected boil-off amount
Transfer losses from receiving vessel	0.1% of delivered LH_2 (peak 2 kg/hr) – top fill for a vessel operating at low pressure (45 psia or so)
Pre-cooling of LH_2 pump	1 kg from 50 K, per LH_2 pump (peak 2 kg/hr)
LH_2 pump utilization	700 bar: 0.6 kg/hour if high utilization, 3 kg/hour if low 350 bar: 0.01 kg/hour if high utilization, 1 kg/hour if low
LH_2 pump idling/warming up	0.5 kg/hr (peak 0.8 kg/hr)

Table 5: Estimation of the boil-off losses as a function of station size, for a LH_2 pump with a 100 kg/hr nominal flow rate, whose boil-off performances have been measured at LLNL, dispensing H_2 to **700 bar** through direct fill.

Station size	**Peak flow over 1 hr**	**number of pumps**	**Losses from pump pre-cooling**	**Total pumping time per day**	**Total idling time per day**	**%pump utilization**	**Total losses from pumps utilization, per day**	**Total losses from pumps idling, per day**	**Size of Dewar**	**Transfer losses**	**Losses for each delivery (every 2 days)**	**Losses per day**	**% losses per kg of LH_2 delivered**
kg/day	*kg*	-	*kg*	*hours*	*hours*	*%*	*kg*	*kg*	*kg*	*kg*	*kg*	*kg*	*%*
100	8	1	1.1	1	23	4	3	12	200	0.2	32	16	16.2
200	16	1	1.1	2	22	8	4	9	400	0.4	28	14	6.9
300	23	1	1.1	3	21	13	4	8	600	0.6	27	14	4.5
400	31	1	1.1	4	20	17	4	7	800	0.8	24	12	3.1
500	39	2	1.7	5	43	10	4	7	1,000	1	27	14	2.7
600	47	2	1.7	6	42	13	5	16	2,000	1.2	46	23	3.8
700	55	2	1.7	7	41	15	5	14	3,000	1.4	43	22	3.1
800	62	2	1.7	8	40	17	6	13	3,600	1.6	43	22	2.7
900	70	2	1.7	9	39	19	6	13	4,200	1.8	43	21	2.4
1000	78	3	2.2	10	62	14	7	13	4,800	2	47	23	2.3
1200	94	3	2.2	12	60	17	9	18	5,400	2.4	60	30	2.5
1400	109	3	2.2	14	58	19	10	18	6,000	2.8	61	31	2.2
1600	125	4	2.6	16	80	17	11	22	6,600	3.2	73	37	2.3
1800	140	4	2.6	18	78	19	12	21	7,200	3.6	75	38	2.1
2000	156	5	3.0	20	100	17	12	25	7,800	4	85	42	2.1
2200	172	5	3.0	22	98	18	14	29	8,400	4.4	96	48	2.2
2400	187	5	3.0	24	96	20	15	28	9,000	4.8	97	49	2.0
2600	203	6	3.3	26	118	18	16	31	9,600	5.2	106	53	2.0
2800	218	6	3.3	28	116	19	17	31	10,200	5.6	108	54	1.9
3000	234	7	3.5	30	138	18	18	31	10,800	6	112	56	1.9
4000	312	9	3.8	40	176	19	24	36	11,400	8	136	68	1.7
5000	390	11	3.7	50	214	19	30	41	12,000	10	158	79	1.6

Table 6: Estimation of the boil-off losses as a function of station size, for a LH_2 pump with a 100 kg/hr nominal flow rate, whose boil-off performances have been measured at LLNL, dispensing H_2 to **350 bar** through direct fill.

Station size	**Peak flow throughput**	**number of pumps**	**Losses from pump pre-cooling**	**Total pumping time per day**	**Total idling time per day**	**%pump utilization**	**Total losses from pump utilization, per day**	**Total losses from pump idling, per day**	**Size of Dewar**	**Transfer losses**	**Losses for each delivery (every 2 days)**	**Losses per day**	**% losses per kg of LH_2 delivered**
kg/day	*kg/hr*	-	*kg*	*hours*	*hours*	*%*	*kg*	*kg*	*kg*	*kg*	*kg*	*kg*	*%*
100	8	1	1.1	1	23	4	1.0	12	200	0.2	28	14	14.2
200	16	1	1.1	2	22	8	1.3	7	400	0.4	20	10	4.9
300	23	1	1.1	3	21	13	1.1	6	600	0.6	17	9	2.9
400	31	1	1.1	4	20	17	0.7	4	800	0.8	13	7	1.7
500	39	2	1.7	5	43	10	0.8	4	1000	1	15	7	1.5
600	47	2	1.7	6	42	13	1.4	13	1200	1.2	33	17	2.8
700	55	2	1.7	7	41	15	1.1	10	1400	1.4	28	14	2.0
800	62	2	1.7	8	40	17	1.4	9	1600	1.6	26	13	1.6
900	70	2	1.7	9	39	19	0.7	8	1800	1.8	23	11	1.3
1000	78	3	2.2	10	62	14	1.5	8	2000	2	25	12	1.2
1200	94	3	2.2	12	60	17	0.5	13	2400	2.4	35	17	1.4
1400	109	3	2.2	14	58	19	0.5	12	2800	2.8	32	16	1.1
1600	125	4	2.6	16	80	17	0.7	15	3200	3.2	40	20	1.2
1800	140	4	2.6	18	78	19	0.8	14	3600	3.6	38	19	1.0
2000	156	5	3.0	20	100	17	1.0	13	4000	4	39	19	1.0
2200	172	5	3.0	22	98	18	1.5	13	4400	4.4	39	19	0.9
2400	187	5	3.0	24	96	20	1.3	12	4800	4.8	37	18	0.8
2600	203	6	3.3	26	118	18	1.5	14	5200	5.2	42	21	0.8
2800	218	6	3.3	28	116	19	1.7	13	5600	5.6	42	21	0.7
3000	234	7	3.5	30	138	18	1.7	15	6000	6	46	23	0.8
4000	312	9	3.8	40	176	19	2.6	15	8000	8	51	25	0.6
5000	390	11	3.7	50	214	19	4.0	15	10000	10	56	28	0.6

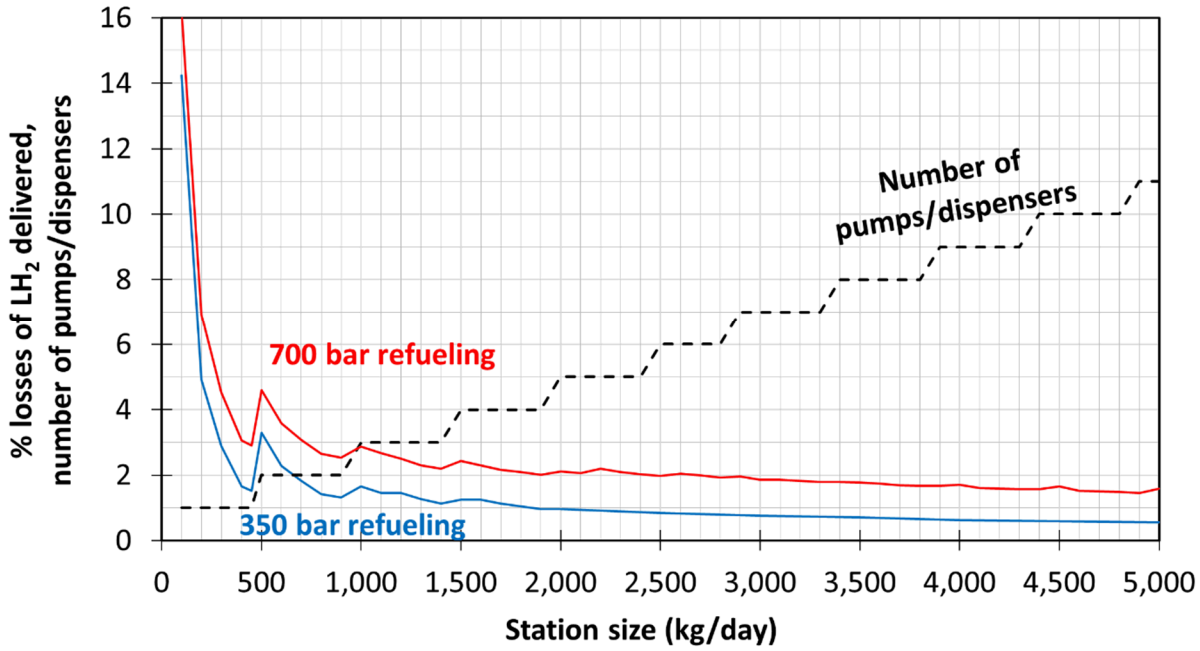

Figure 32: %losses of LH_2 delivered as a function of station size, based on **Table 5** and **Table 6**. The number of pumps/dispensers assumed for each station size is also shown.

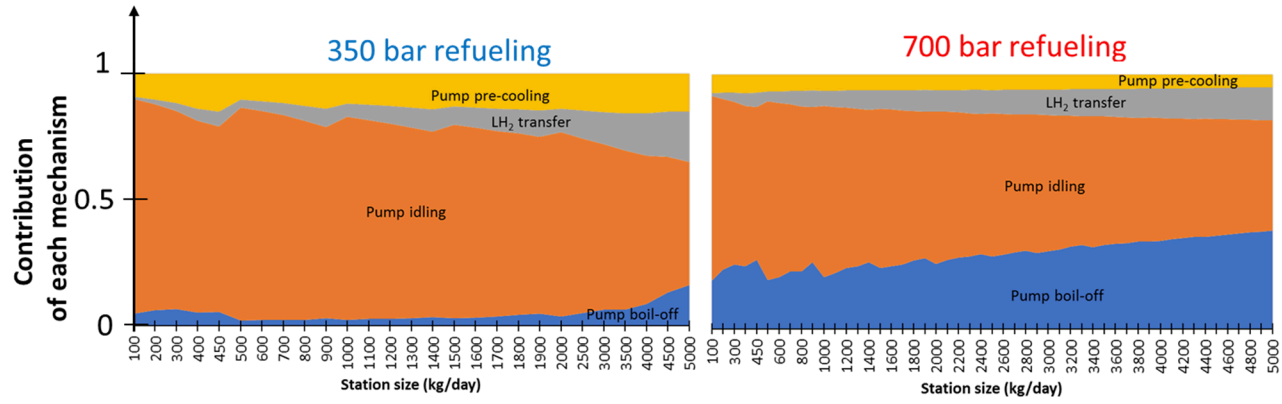

Figure 33: Relative contribution of boil-off mechanisms for 350 and 700 bar refueling (left and right figures, respectively).

6. Boil-off recovery solutions

Some boil-off losses are inherent to the design of the system (e.g. losses during pump vessel cool down) or thermodynamically limited (e.g. compression heat from the LH_2 pump), and thus cannot eliminated. Boil-off recovery solutions should be implemented in order to reduce the economic impact of those losses to the end-user. Those losses could be captured and stored at the refueling station, they could be re-liquefied, or they could be used through a fuel cell. The techno-economic relevance of those different options should be evaluated on a case-by-case basis, and high-level guidelines are given below.

Based on the section above, peak flow rates of up to 2-3 kg/hour of boil-off would need to be captured, as measured at LLNL facility. If a better cryogenic engineering design may be achieved, a 2 kg/hour peak and 0.6 kg/hr nominal recovery flow rate was targeted.

It is considered that mitigation solutions should avoid relying on additional supplies such as (L)N_2 or (L)Helium, should have positive operational expenses (the energy used to recover the boil-off losses should have a lower cost than the boil-off itself), and should provide "reasonable" payback period, like 3 to 5 years. A few parameters need to be considered to evaluate the payback period: electricity consumption (in kWh/kg H_2), expected cost of electricity (in \$/kWh), initial installed capital expenditure, maintenance costs (in general, expressed as % per year of the initial installed capital expenditure), expected cost of H_2 (in \$/kgH_2), and of course the amount of H_2 recovered. **Figure 34** and **Figure 35** illustrate those relationships for 2 constant boil-off flow rates, 0.6 and 2 kg/hour, and for an expected payback period of 3 years. As the costs of hydrogen and electricity decrease, the initial capital expenditure needs to be lower and lower for the implemented solution to make sense.

Various recovery solutions are discussed next. The option of flaring the boil-off H_2 was not investigated.

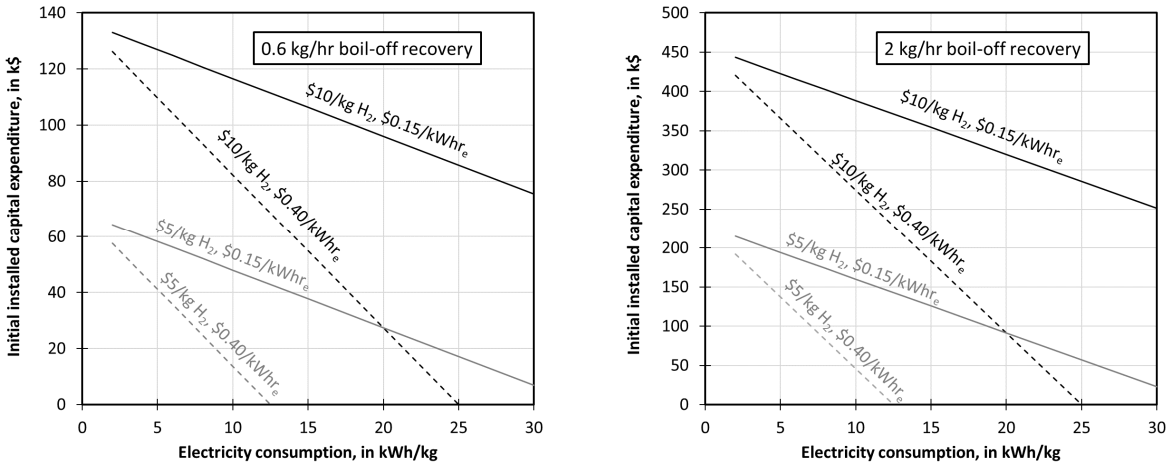

Figure 34: Relationship between maximum electricity consumption and initial installed capital expenditure for a 0.6kg/hr (left) and 2 kg/hr (right) boil-off recovery system that would enable a 3 year payback period, for 2 different costs of hydrogen (\$5 and \$10 kg/H_2) and electricity (\$0.15 and \$0.4/kWh), assuming a yearly cost of operation and maintenance of 5% of the initial installed capital expenditure.

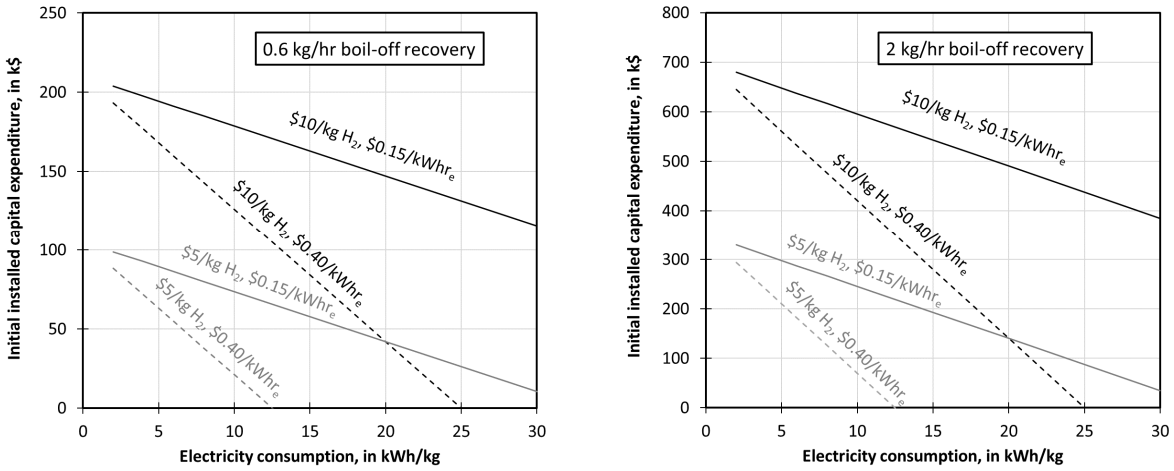

Figure 35: Relationship between maximum electricity consumption and initial installed capital expenditure for a 0.6kg/hr (left) and 2 kg/hr (right) boil-off recovery system that would enable a 5 year payback period, for 2 different costs of hydrogen ($5 and $10 kg/$H_2$) and electricity ($0.15 and $0.4/kWh), assuming a yearly cost of operation and maintenance of 5% of the initial installed capital expenditure.

6.1. Capturing the vented H_2 using a compressor

Capturing the vented H_2 may be one of the first solution that comes to mind when considering mitigation options. H_2 is generally vented around 45 psia and at temperatures between 24 and 28 K. Given the low density of the vented H_2, it is necessary to compress it to then store it in pressure vessels, insulated or not. The captured H_2 could be used for secondary application at the refueling station (e.g. through a fuel cell) or could be stored in existing pressure vessels in the cascade to be eventually dispensed to the vehicle. The latter option is available only when non-direct fills are conducted, which may not be ideal for a large throughput station. Also, re-liquefying from room temperature the stored H_2 is not considered as economically viable. At last, the stored boil-off losses could also be sold to third parties if such a market is available in the area where the refueling station is located. For reference, an inexpensive 2,000 psi industrial gas bottle contains ~200 ft^3 H_2 at atmospheric conditions, thus around 0.5 kg of H_2, which means that 15 (for 100 kg/day station) to 77 (for 6,000 kg/day station) bottles would need to be filled and handled each day… This could be avoided by using a larger outlet pressure, but the associated costs would then dramatically increase. In this work, only the economics of the recovery system (i.e. the compressor) are discussed, not how the recovered H_2 is handled downstream.

A few options exist concerning the type of compressor that can be used: electro-chemical, metal hydride, diaphragm, reciprocating, rotary, centrifugal... The relevance of a design highly depends on the required performances (flow rate, output pressure) and the associated costs (electricity consumption, maintenance, installation, initial capital). One difficulty in evaluating their relative benefits is that those compressors have different level of maturity, and only a handful have been developed for the boil-off recovery application.

Rosso and Golben [41] presented a design to capture boil-off at the Kennedy Space Center with a metal hydride compressor for subsequent reliquefication. They estimated that 1.5 million gallons of liquid hydrogen could be recovered assuming 170 off-loading operations per year. Proof-of-concept testing using

$LaNi_{4.6}Al_{0.4}$T-88860-2 demonstrated low pressure absorption at more than adequate rates. Payback time of less than 3 years were projected, although no details were given concerning that result. A more recent study [42] detailed a La and Ni metal hydride tank specifically designed to capture boil-off gases from LH_2. No details on the economics are given. At last, 2 very thorough papers ([43] and [44]) present various metal hydride compressors applications for hydrogen , including isotope handling, cryogenics/space, utilization of low-grade heat, thermally driven actuators, and industrial-scale. Even though economic estimations are difficult to obtain, [44] mentions a metal hydride compressor prototype (10-100 bar, 0.42 m^3/hour) estimated to cost around $23,000, to be compared with a $27,000 PPI compressor equivalent. Another cost estimate of $32,000-$39,000 is given for a 3-150 bar, 10 m3/hour metal hydride compressor. That cost was used in the following economics analysis.

Electrochemical compressors represent an interesting solution for compression, as it relies on a more efficient process to compress H_2, typically using a PEM approach ([45], [46], [47]). This technology is being developed by a handful of companies, such a Fuel Cell Energy, Nuvera, Skyre, Proton… Projections from Strategic Analyses [48] were used to estimate expected capital and operating expenditures.

Mechanical compressors represent a much more mature solution that metal hydride and electrochemical compressors. After discussing with a few vendors concerning the application, a hydraulically driven intensifier style compressor technology was identified as being the most adequate.

Table 7: Summary comparison of H_2 compressor designs for boil-off capture (0.6 to 2 kg/hour)

	Inlet pressure	**Outlet pressure**	**Commercial availability**	**Electricity consumption**	**Flow rate**
Mechanical	45 psia	290-1500 psia	Yes	1.8 to 5.2 kWh/kg	0.6 to 2 kg/hr
Metal hydride	45 psia	2000 psia	R&D (not developed for low temperature)	N/A	0.8 kg/hr
Electrochemical	45 psia	500-1000 psi	Near-commercial	8.6 kWh/kg	2 kg/hr

Figure 36 summarizes capital cost and electricity consumption performances for compressors, relative to hydrogen and electricity cost. The cost of storage is not included. Although some disparities exist, mechanical and electrochemical compressors could make economic sense even under conservative assumptions for H_2 and electricity costs (less than $5/kg H_2 and more than $0.40/kWh electricity). Metal hydride compressors could also potentially represent a good solution, even though their operating costs are not fully understood yet. Indeed, metal hydride compressors typically need heat, not electricity, to function.

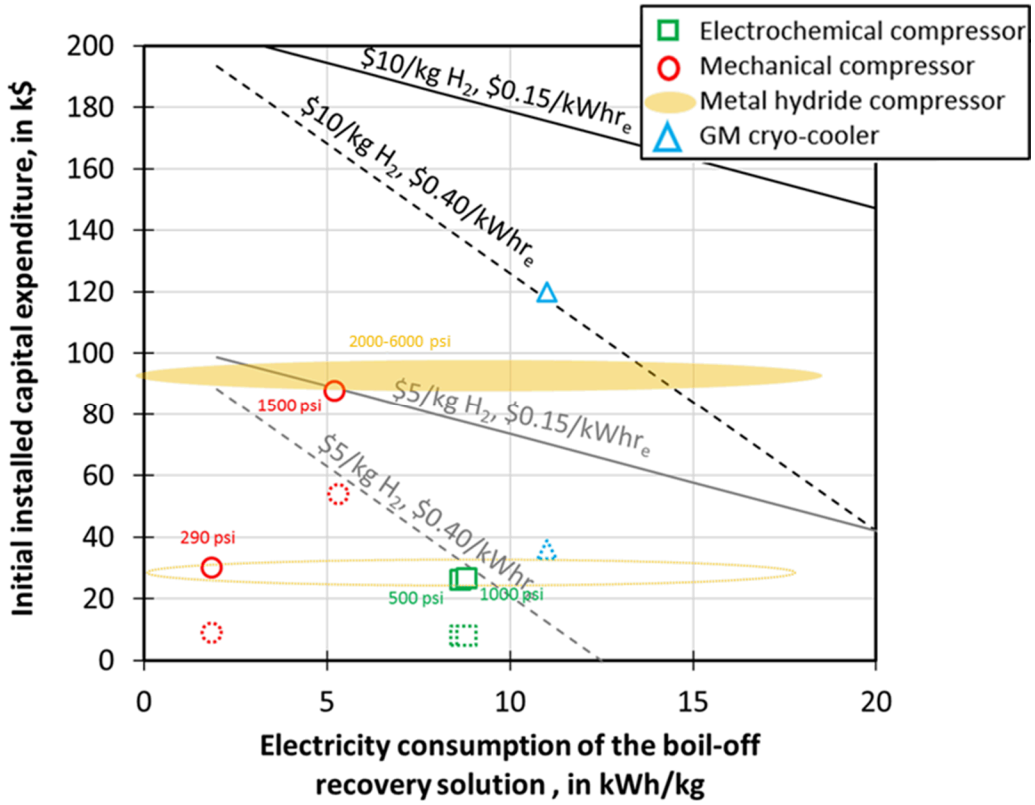

Figure 36: Relationship between maximum electricity consumption and initial installed capital expenditure for boil-off recovery system that would enable a 5 year payback period, for 2 different costs of hydrogen ($5 and $10 kg/$H_2$) and electricity ($0.15 and $0.40/kWh), assuming a yearly cost of operation and maintenance of 5% of the initial installed capital expenditure. Symbols show the expected initial installed capital expenditure and electricity consumption for 4 different boil-off recovery solution: electrochemical compressor (green squares), mechanical compressors (red circles), metal hydride compressor (orange), and GM cryo-cooler (blue triangle). 2 types of symbols are shown, continuous and dotted lines; which account for a system designed for peak (2 kg/hr) and nominal (0.6 kg/hr) flow rates, respectively. Outlet pressures are also reported.

6.2.Cryo-refrigeration of the head space

Re-liquefying the boil-off H_2 can represent an interesting option as the boil-off H_2 is already cold and still in its *para*-hydrogen isomer state. This solution would ensure that all the H_2 ends up being delivered to the FCEV (no secondary utilization). This could be performed directly in the vessel or using another vessel, although the second solution would represent extra cost. A zero loss solution has recently been demonstrated by NASA (Ground Operations Demonstration Unit for Liquid Hydrogen, or GODU-LH_2) in an horizontal 33,000 gallon Dewar, using a closed-loop Helium refrigeration system capable of 880-390 W cooling at 20 K (depending whether a LN_2 pre-cooling is used or not), with a heat exchanger installed directly inside the Dewar [28]. Refrigeration solutions include a Brayton cycle unit [28], a Stirling cycle [49], a Linde-Hampson cycle [50], a Gifford-McMahon cryo-cooler [51] or a linear-drive pulse tube cooler [52]. Thermoacoustic ([53], [54], [55]) and magnetic ([56], [57]) refrigeration based technologies are not included here as they are considered not mature enough.

Given our re-liquefaction needs (0.6 to 2 kg/hour, thus ~ 100 to 170 Watts at 23-25 K) and based discussions with multiple vendors, it appears that a Gifford-McMahon cryo-cooler is the most adequate design. **Figure**

36 shows the economic relevance of using a cryo-cooler, see blue triangles. This solution does not perform as well as compressor-based solutions although it would still make sense for low cost hydrogen ($5/kg H_2 or so) as long as the electricity is affordable (~$0.20/kWh or less). The advantage of using a cryo-cooler is that the boil-off losses are re-liquefied into high value LH_2 and that the footprint can be very small (integration onto existing vessels and no need for secondary equipment to handle captured boil-off).

6.3. Running the boil-off H_2 through a fuel cell

Using boil-off H_2 through a fuel cell to produce electricity poses an interesting challenge. The produced electricity could be used at the refueling station, to run partially or entirely the liquid pump or the compressor, or ancillary equipment such as air condition units or cooling system for the pump/compressor. The cost advantage of using electricity from the fuel cell as opposed from the grid can be first simply approached in terms of breakeven costs between electricity from the grid and H_2: assuming a 50% energy efficiency for a fuel cell and neglecting capital and operational expenses for the fuel cell and connection cost for the grid, it makes economic sense to use electricity from the fuel cell only if the cost of the H_2, A, is equal to or lower than the cost of electricity from the grid, B, such as A [$/kg] /(0.5* LHV_$H_2$ [kWh/kg]) ≤ B [$/kWh], where LHV_$H_2$ is the Lower Heating Value of H_2, equal to 33 kWh/kg. This relationship is illustrated on **Figure 37**.

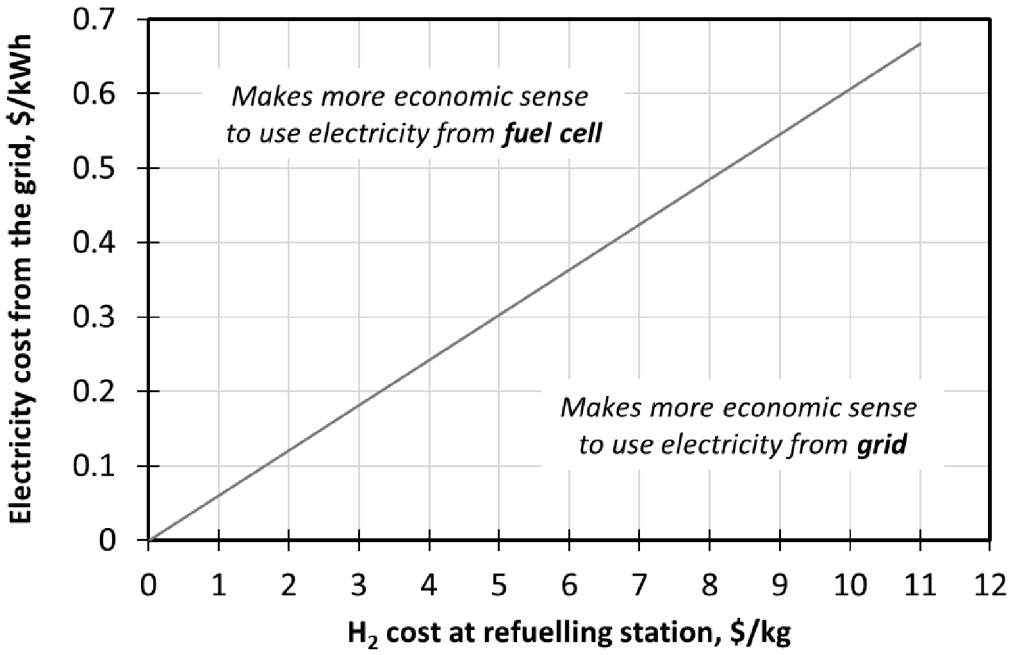

Figure 37: Illustration of the trade-off between H_2 and electricity (from the grid) cost, assuming a 50% efficient fuel cell and no capital nor operational expenses.

The peak and boil-off rate used in this paper (2 kg/hr) would need to feed a 33 kW fuel cell system (assuming a 50% energy efficiency) to be able to capture all the boil-off losses at the refueling stations. It is further assumed that all the produced electricity from boil-off is used to power the pump when in used and is sold to the grid at a $0.02/kWh rate when the pump is unused. The main benefit of running the boil-off through the fuel cell is thus to pay less electricity for using the pump/compressor. A payback period can

thus be calculated as a function of station size and cost of electricity, using the assumptions presented earlier – see section 5. This relationship is shown on **Figure 38**, assuming $2000/kW initial installed capital expenditure for the 33 kW fuel cell. If the electricity cost from the grid is high enough ($0.40/kWh), it would make sense to rather use the electricity produced by the fuel cell to power the pump(s), with a payback period of less than 5 years for station larger than ~2,000 kg/day.

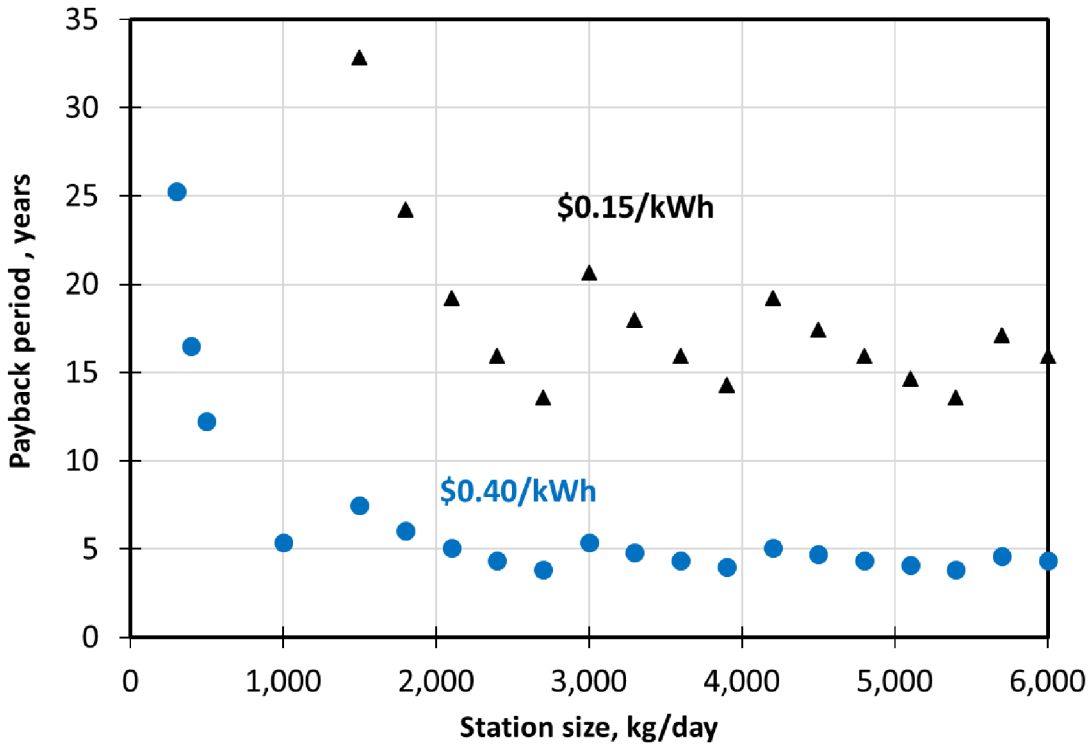

Figure 38: Payback period for a 33 kW fuel cell (assumed cost: $66,000, i.e. $2000/kW) used to capture boil-off at a refueling station, assuming 5% CAPEX yearly maintenance, and $0.02 selling cost to the grid when the pump is unused; as a function of station size and for different costs of electricity typically bought from the grid ($0.15 and $0.40/kWh).

6.4.Summary of mitigation solutions

Recovery solutions can be used to capture all the boil-off at a LH_2 based hydrogen station, and those solutions come with an extra cost for the end-user. Integrating those costs as a function of equivalent amount of H_2 paid enables estimate the effective boil-off. **Figure 39** shows a comparison of the different recovery solution discussed above. That comparison assumes that all the boil-off recovered is eventually sold to a customer as hydrogen, except for the fuel cell solution where the boil-off is converted to electricity. The metal hydride compressor solution is not represented as the cost for the end-user is not clearly understood. All solutions enable savings as compared to the baseline (left black bars), even under conservative assumptions (high cost of hydrogen, low cost of electricity). Those effective boil-off values are a strong function of the efficiency of the solution with regards to electricity consumption. A GM cryo-cooler with typically high electricity costs (11 kWh/kg) will provide less savings than an electrochemical or mechanical compressor.

Here again those comparisons do not consider the associated costs with storing the captured boil-off hydrogen.

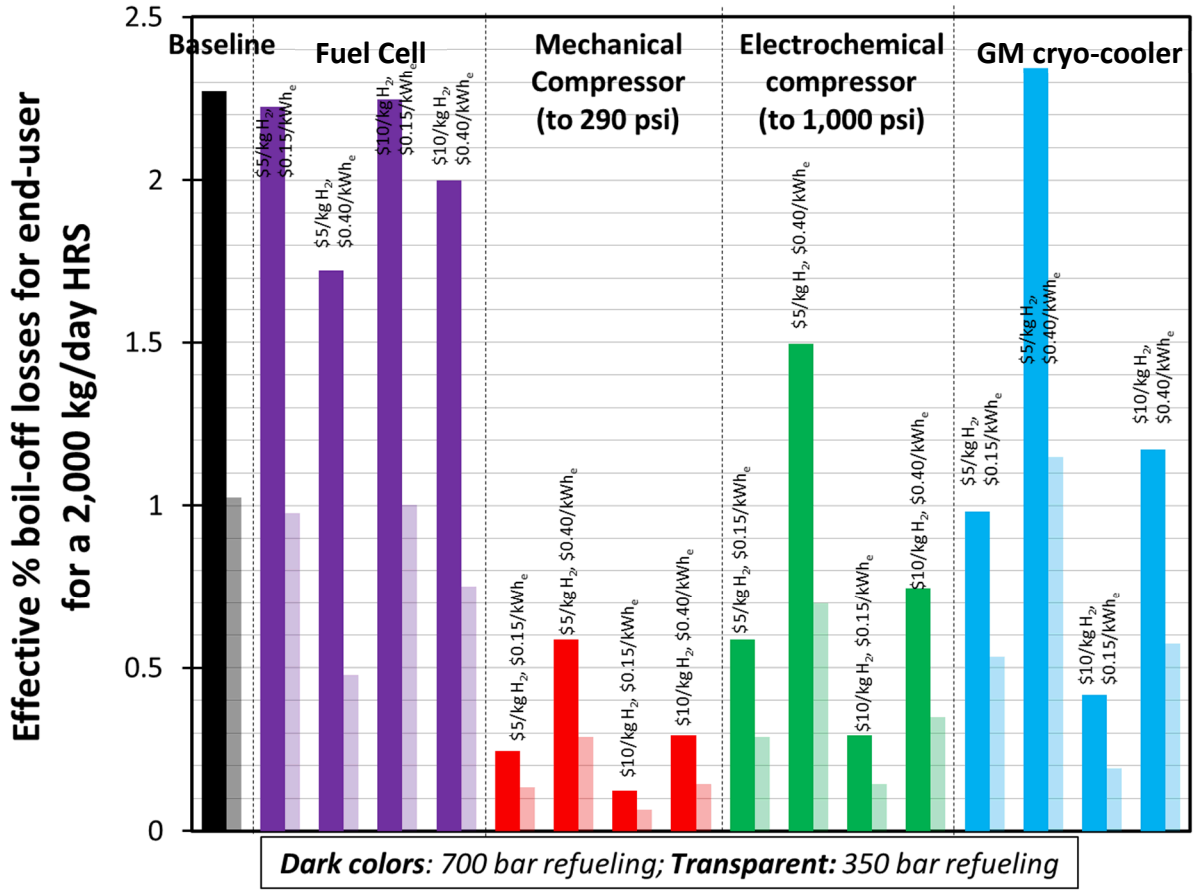

Figure 39: Effective boil-off losses for a 2,000 kg/day hydrogen refueling station assuming different recovery mechanisms, for 2 different dispensing pressures: 700 bar (dark colors) and 350 bar (transparent).

Conclusions

In this work, a 0D thermodynamics dynamical transfer model for LH_2 rocket was modified to simulate the transfer along the LH_2 pathway for utilizing H_2 as a transportation fuel for FCEV. The LH_2 pathway considered here goes from the trailer refill at the H_2 liquefaction plant to the dispensing at the hydrogen refilling station, and thus the main components are: the LH_2 trailer, the LH_2 stationary vessel, and the LH_2 pump. Outcomes from this work could be applied to other dispensing configurations such as a compressor that would take vaporized LH_2 at its inlet. The main goal of this effort is to understand and quantify the boil-off mechanisms at the different steps of the LH_2 pathway to be able to reduce or even eliminate them. The results and boundary conditions for the model were informed by the industry's practices, so that relevant scenarios could be analyzed.

The experimental data needed to perform model validation (such as temperatures variations inside the vessels, or flow rates, for the actual equipment that was simulated) were not readily available. Nonetheless, a few verification steps were taken to make sure the physical behaviors were captured and to calibrate the heat transfer with the environment, e.g. using inventory variations from a 3,300 gallon LH_2 tank installed at Lawrence Livermore National Laboratory (Livermore, CA).

- It was estimated that about 3.3% of the liquid entering the trailer during the refill at the liquefaction terminal was vented as boil-off. This vapor is almost always captured and re-circulated back into the liquefaction process. Therefore, the boil-off during the refill at the liquefaction terminal can be assumed negligible (not accounting losses during piping dis-connection), although it certainly has an impact on the overall energy efficiency of the liquefaction process.

- The LH_2 trailer generally leaves the plant at a reasonably low pressure (20 psia or so). Based on the CFR/DOT regulations for One Way Travel Time (Code of Federal Regulations, title 49 173.318(g) [20]) , the insulation of the LH_2 trailer is such that it would take a long time (at least 110 hours for a full trailer) to reach the pressure relief set value. This pressurization time can be regarded as larger than what a trailer would typically experience when delivering to hydrogen refilling stations. As a result, it was assumed that no venting was occurring during the travel from the liquefaction plant to the hydrogen refueling station. Additionally, based on the One-Way Travel Time markings, it was estimated that the typical heat transfer for a near full trailer was about 270 Watts. This value was used in subsequent simulations.

- The model was used to estimate the heat transfer profile of the 3,300 gallon LH_2 tank located at Lawrence Livermore National Laboratory (Livermore, CA), based on the variations of inventory due to heat transfer with environment alone recorded over several months. It was found that the heat transfer profile for the tank was not an important function of the outside environment temperature but was rather dependent on the level of fill, varying from 70 Watts near full to 30 Watts when empty. It was also shown that some temperature gradients may exist across the vessel (this aspect may be revisited in the future by considering stratification) and that the density of the liquid was slightly below the expected saturation density.

- The transfer from the trailer to the stationary LH_2 tank was simulated and the compression of the vapor space (or ullage) in the receiving vessel was identified as the main root-cause for transfer losses. It was shown that the transfer losses were strongly dependent on the initial pressure in the receiving vessel, from 2 to 10% of the transferred mass between 20 and 80 psia, when using bottom fill only.

The following can be summarized concerning boil-off losses along the LH_2 pathway:

- The venting losses from the trailer after the transfer at the refueling station are not a significant source of losses as long as the trailer is operated as required by the CFR/DOT regulations. Under most scenarios, the trailer is not required to be de-pressurized, and this is even more true when the operating pressure of the receiving vessel is relatively low. Trailer depressurization may occur if only small quantities are delivered from a full trailer (please refer to section 4.1 for a full discussion on the topic), or under non-routine case specific scenarios (e.g. valves on the trailer are leaking under pressure and thus require full depressurization).

- Transfer losses from the receiving vessel (e.g. LH_2 tank at the station) are likely the most significant along the LH_2 pathway. They can be mitigated by reducing the relief set pressure of the vessel. Top fill is probably the most effective way to reduce those transfer losses, although more understanding of the underlying physics may be needed, to understand and take better advantage of the injection method. Experimental measurements in the literature and collected at LLNL's facility suggest that close to no-vent fill could indeed be achieved. Using a low pressure LH_2 transfer pump between the trailer and the receiving vessel would lower the temperature of the incoming LH_2 and thus reduce transfer losses.

- If the transfer losses from the receiving vessel during a delivery can be strongly reduced, the boil-off along the LH_2 pathway, up to and including dispensing, is mostly due to the LH_2 pump utilization and idling. If using a compressor, more significant losses may occur since the stationary storage operates at a larger pressure, thus venting may be necessary before transfer.

- Based on experimental data, results from the model, and extrapolating for refueling stations of various sizes, it can be shown that boil-off losses can vary from 15% of delivered LH_2 for a 100 kg/day, down to 5% at 400 kg/day, and down to less than 2% for stations above 1,800 kg/day. Less boil-off is to be expected for LH_2 pumps dispensing at 350 bar, so that less than 0.7% can be expected above 1,800 kg/day station capacities.

- Capturing those boil-off losses to offset the associated extra cost for the end-user makes sense from an economic perspective only if the cost of H_2 is large when compared to electricity used, and if the initial capital expenditures are reasonable. Compressors may be a good option but the final application of the recovered boil-off H_2 is not clear. An interesting case can be made to use a cryo-cooler to re-liquefy the vapor H_2 in the pump vessel or in the stationary vessel, although the capital expenditure remains high now. Alternatively, it may also make sense to use a stationary fuel cell to convert the boil-off losses into electricity to power (partially) the pump, provide power to auxiliary equipment, or even re-sell the electricity produced.

Follow-up efforts concerning the evaluation/mitigation of boil-off along the LH_2 pathway should include analysis of no-vent fills (no transfer loss from receiving vessel) through CFD modelling and experimental measurements in order to confirm the relevance of the approach, validation of the MATLAB code presented in this document, and development of recovery solutions that may be better suited than the ones presented here.

Acknowledgements

This work was sponsored by the US Department Of Energy, Fuel Cell Technologies Office, Program Managers: Erika Gupta, Neha Rustagi, whose support is gratefully acknowledged. Very fruitful interactions with the following individuals should also be mentioned as they were critical contributions to this work: Al Brugunder (Praxair), Matt Moran (Isotherm Energy), Erik Tudbury (Linde), Kyle McKeown (Linde), Willy Reese (Linde), Bill Notardonato (NASA), Amgad Elgowainy (ANL). The work was performed under the auspices of the U.S. Department of Energy by Lawrence Livermore National Laboratory under Contract DE-AC52- 07NA27344.

Disclaimer

References

[1] K. Reddi, M. Mintz, A. Elgowainy, and E. Sutherland, "Challenges and Opportunities of Hydrogen Delivery via Pipeline, Tube-Trailer, LIQUID Tanker and Methanation-Natural Gas Grid," in *Hydrogen Science and Engineering : Materials, Processes, Systems and Technology*, D. Stolten and B. Emonts, Eds. Wiley-VCH Verlag GmbH & Co. KGaA, 2016, pp. 849–874.

[2] G. Petitpas and S. M. Aceves, "The isentropic expansion energy of compressed and cryogenic hydrogen," *International Journal of Hydrogen Energy*, vol. 39, no. 35, pp. 20319–20323, Dec. 2014.

[3] S. M. Aceves *et al.*, "High-density automotive hydrogen storage with cryogenic capable pressure vessels," *International Journal of Hydrogen Energy*, vol. 35, no. 3, pp. 1219–1226, Feb. 2010.

[4] S. M. Aceves, G. Petitpas, F. Espinosa-Loza, M. J. Matthews, and E. Ledesma-Orozco, "Safe, long range, inexpensive and rapidly refuelable hydrogen vehicles with cryogenic pressure vessels," *International Journal of Hydrogen Energy*, vol. 38, no. 5, pp. 2480–2489, Feb. 2013.

[5] "Hydrogen Delivery Infrastructure Analysis." [Online]. Available: http://hdsam.es.anl.gov/. [Accessed: 28-Dec-2017].

[6] California Environmental Protection Agency Air Resources Board, "Staff report: Initial statement of reasons, Advanced Clean Cars, 2012 Proposed Amendments To The Clean Fuels Outlet Regulation," Dec. 2011.

[7] "AC Transit fuel cell bus sets 25 000 h operating record," *Fuel Cells Bulletin*, vol. 2017, no. 8, p. 3, Aug. 2017.

[8] M. Gardiner, "Energy requirements for hydrogen gas compression and liquefaction as related to vehicle storage needs, DOE Hydrogen Program Record # 9013," 26-Oct-2009. [Online]. Available: http://www.hydrogen.energy.gov/pdfs/9013_energy_requirements_for_hydrogen_gas_compression.pdf.

[9] V. V. Osipov and C. B. Muratov, "Dynamic condensation blocking in cryogenic refueling," *Applied Physics Letters*, vol. 93, p. 224105, Dec. 2008.

[10] V. V. Osipov, M. J. Daigle, C. B. Muratov, M. Foygel, V. Smelyanskiy, and M. D. Watson, "Dynamical Model of Rocket Propellant Loading with Liquid Hydrogen," *Journal of Spacecraft and Rockets*, vol. 48, no. 6, pp. 987–998, 2011.

[11] V. Osipov and B. Muratov, "Dynamic condensation blocking in cryogenic refueling," *Applied Physics Letters*, vol. 93, pp. 224105–224105, Jan. 2009.

[12] M. Daigle, M. Foygel, and V. Smelyanskiy, "Model-based diagnostics for propellant loading systems," in *2011 Aerospace Conference*, 2011, pp. 1–11.

[13] V. Osipov, B. Muratov, M. Daigle, M. Foygel, V. Smelyanskiy, and A. Patterson-Hine, *Dynamical Physics Model of Nominal and Faulty Operational Modes of Propellant Loading (Liquid Hydrogen): From Space Shuttle to Future Missions*. 2010.

[14] P. N. ESTEY, D. H. LEWIS, and M. CONNOR, "Prediction of a propellant tank pressure history using state space methods," *Journal of Spacecraft and Rockets*, vol. 20, no. 1, pp. 49–54, 1983.

[15] C. N. TORRE, J. A. WITHAM, E. A. DENNISON, R. C. MCCOOL, and M. W. RINKER, "Analysis of a low-vapor-pressure cryogenic propellant tankage system," *Journal of Spacecraft and Rockets*, vol. 26, no. 5, pp. 368–378, 1989.

[16] L. D. Landau and E. M. Lifshitz, *Fluid Mechanics, Second Edition: Volume 6*, 2 edition. Amsterdam u.a: Butterworth-Heinemann, 1987.

[17] E. W. Lemmon, M. L. Huber, and M. O. McLinden, "NIST Standard Reference Database 23: Reference Fluid Thermodynamic and Transport Properties-REFPROP." National Institute of Standards and Technology, Standard Reference Data Program, , Gaithersburg, 2007.

[18] "http://trc.nist.gov/refprop/LINKING/Linking.htm."

[19] E. D. Marquardt, J. P. Le, and R. Radebaugh, "Cryogenic Material Properties Database," in *Cryocoolers 11*, Keystone, Co, 2000.

[20] "Electronic Code of Federal Regulations, https://www.ecfr.gov/."
[21] S. C. Honkonen and D. J. Chato, "Comparison of Liquid Hydrogen no-Vent Fill Test Data with Analytic Models," in *Advances in Cryogenic Engineering*, Kittel P., vol. 39, Boston, MA: Springer, 1994.
[22] M. E. N. Moran, "Hydrogen no-vent fill testing in a 1.2 cubic foot (34 liter) tank," Oct. 1991.
[23] M. E. N. Moran, "Hydrogen no-vent fill testing in a 5 cubic foot (142 liter) tank using spray nozzle and spray bar liquid injection," presented at the Joint Propulsion Conference and Exhibit, 6-8 Jul. 1992, United States, 1992.
[24] D. J. Chato, "Ground testing for the no-vent fill of cryogenic tanks - Results of tests for a 71 cubic foot tank," 01-Jun-1993.
[25] W. J. C. Taylor, "Comparing the results of an analytical model of the no-vent fill process with no-vent fill test results for a 4.96 cubic meters (175 cubic feet) tank," presented at the Joint Propulsion Conference and Exhibit, 6-8 Jul. 1992, United States, 1993.
[26] W. J. C. Taylor, "Improved thermodynamic modeling of the no-vent fill process and correlation with experimental data," presented at the Thermophysics Conference, 24-26 Jun. 1991, United States, 1991.
[27] J. C. R. Aydelott, "Technology requirements to be addressed by the NASA Lewis Research Center Cryogenic Fluid Management Facility program," presented at the Joint Propulsion Conf., 8-10 Jul. 1985, United States, 1985.
[28] W. U. S. Notardonato, "Zero Boil-Off Methods for Large Scale Liquid Hydrogen Tanks Using Integrated Refrigeration and Storage," presented at the Joint Cryogenic Engineering Conference and International Cryogenic Materials Conference 2017, Madison, WI, United States, 2017.
[29] W. Notardonato, "KEA-144: Final Results of the Ground Operations Demonstration Unit for Liquid Hydrogen (GODU-LH_2) Project," 28-Mar-2017.
[30] W. U. J. Notardonato, "Ground Operations Demonstration Unit for Liquid Hydrogen Initial Test Results," presented at the Cryogenic Engineering Conference/International Cryogenic Materials Conference, Tuscon, AZ, United States, 2015.
[31] W. U. S. Notardonato, "Large Scale Production of Densified Hydrogen Using Integrated Refrigeration and Storage," presented at the Joint Propulsion Conference, 10-12 Jul. 2017, United States, 2017.
[32] Y. Kim, C. Lee, J. Park, M. Seo, and S. Jeong, "Experimental investigation on no-vent fill process using tetrafluoromethane (CF4)," *Cryogenics*, vol. 74, pp. 123–130, Mar. 2016.
[33] K. J. Kim, L. Jin, Y. Kim, and S. Jeong, "Experimental Investigation on No Vent Fill Process of Cryogenic Liquid," in *ISOPE-I-17-360*, ISOPE, 2017.
[34] L. Jin, C. Park, H. Cho, C. Lee, and S. Jeong, "Experimental investigation on chill-down process of cryogenic flow line," *Cryogenics*, vol. 79, pp. 96–105, Oct. 2016.
[35] L. Wang, Y. Li, C. Li, and Z. Zhao, "CFD investigation of thermal and pressurization performance in LH_2 tank during discharge," *Cryogenics*, vol. 57, pp. 63–73, Oct. 2013.
[36] L. Wang, Y. Li, F. Zhang, and Y. Ma, "Performance analysis of no-vent fill process for liquid hydrogen tank in terrestrial and on-orbit environments," *Cryogenics*, vol. 72, pp. 161–171, Dec. 2015.
[37] Y. Ma, Y. Li, K. Zhu, Y. Wang, L. Wang, and H. Tan, "Investigation on no-vent filling process of liquid hydrogen tank under microgravity condition," *International Journal of Hydrogen Energy*, vol. 42, no. 12, pp. 8264–8277, Mar. 2017.
[38] K. A. Keefer, "Development and Validation of an Analytical Charge-Hold-Vent Model for Cryogenic Tank Chilldown," Master Thesis, Case Western Reserve University, Cleveland, OH, 2013.
[39] C. Wang, Y. Li, D. Deng, R. Wang, and G. Xie, "Performance Model of the Top Filling Configurations for No-Vent Fills," *Journal of Thermophysics and Heat Transfer*, vol. 25, no. 1, pp. 140–146, Jan. 2011.

[40] T.-P. Chen, "Hydrogen Delivery Infrastructure Options Analysis DOE Award Number: DE-FG36-05GO15032, http://www1.eere.energy.gov/hydrogenandfuelcells/pdfs/delivery_infrastructure_analysis.pdf," .
[41] M. J. Rosso and P. M. Golben, "Capture of liquid hydrogen boil-off with metal hydride absorbers," *Journal of the Less Common Metals*, vol. 131, no. 1, pp. 283–292, Mar. 1987.
[42] A. Nakano *et al.*, "Study on absorption/desorption characteristics of a metal hydride tank for boil-off gas from liquid hydrogen," *International Journal of Hydrogen Energy*, vol. 37, no. 6, pp. 5056–5062, Mar. 2012.
[43] V. A. Yartys *et al.*, "Metal hydride hydrogen compression: recent advances and future prospects," *Appl. Phys. A*, vol. 122, no. 4, p. 415, Apr. 2016.
[44] M. V. Lototskyy, V. A. Yartys, B. G. Pollet, and R. C. Bowman, "Metal hydride hydrogen compressors: A review," *International Journal of Hydrogen Energy*, vol. 39, no. 11, pp. 5818–5851, Apr. 2014.
[45] B. Rohland, K. Eberle, R. Ströbel, J. Scholta, and J. Garche, "Electrochemical hydrogen compressor," *Electrochimica Acta*, vol. 43, no. 24, pp. 3841–3846, Aug. 1998.
[46] P. Bouwman, "Electrochemical Hydrogen Compression (EHC) solutions for hydrogen infrastructure," *Fuel Cells Bulletin*, vol. 2014, no. 5, pp. 12–16, May 2014.
[47] M. Suermann, T. Kiupel, T. J. Schmidt, and F. N. Büchi, "Electrochemical Hydrogen Compression: Efficient Pressurization Concept Derived from an Energetic Evaluation," *J. Electrochem. Soc.*, vol. 164, no. 12, pp. F1187–F1195, Jan. 2017.
[48] "Discussion with Brian James and Daniel De Santis, Strategic Analyses."
[49] "CEA france target Irradiation." [Online]. Available: https://www.stirlingcryogenics.com/en/projects/research/cea-france. [Accessed: 27-Dec-2017].
[50] J. w Pelfrey, "A Low Cost, Self-Acting, Liquid Hydrogen Boil-Off Recovery System," Jun. 2000.
[51] "Gifford-McMahon Cryorefrigerators," *Cryomech*. [Online]. Available: http://www.cryomech.com/cryorefrigerators/gifford/. [Accessed: 27-Dec-2017].
[52] A. L. Johnson, "Reversible Cycle Piston Pulse Tube Cryocooler," in *Cryocoolers 9*, Springer, Boston, MA, 1997, pp. 309–318.
[53] D. B. Chelton, J. W. Dean, and B. W. Birmingham, "Design and Construction of a Liquid Hydrogen Temperature Refrigeration System," U.S. Department of Commerce National Bureau of Standards, 95–24846, 1960.
[54] S. L. GARRETT, J. A. ADEFF, and T. J. HOFLER, "Thermoacoustic refrigerator for space applications," *Journal of Thermophysics and Heat Transfer*, vol. 7, no. 4, pp. 595–599, 1993.
[55] J. Y. Hu, E. C. Luo, S. F. Li, B. Yu, and W. Dai, "Heat-driven thermoacoustic cryocooler operating at liquid hydrogen temperature with a unique coupler," *Journal of Applied Physics*, vol. 103, no. 10, p. 104906, May 2008.
[56] K. Matsumoto, T. Kondo, S. Yoshioka, K. Kamiya, and T. Numazawa, "Magnetic refrigerator for hydrogen liquefaction," *J. Phys.: Conf. Ser.*, vol. 150, no. 1, p. 012028, 2009.
[57] T. Numazawa, K. Kamiya, T. Utaki, and K. Matsumoto, "Magnetic refrigerator for hydrogen liquefaction," *Cryogenics*, vol. 62, no. Supplement C, pp. 185–192, Jul. 2014.

Appendix A: Calibration report for the 3,300 gallon Dewar

CHART STORAGE SYSTEMS DIVISION PLAISTOW, NH 03865

CONTENTS TABLE, MODEL 3300-7-175#

LIQUID HYDROGEN at 30 PSIG

Liquid Density= 4.056 Lb/CuFt. Vapor Density= .235 Lb/CuFt. SCF/Lb= 191.98

GALLONS are at Liquid Density shown. TOTAL is Liquid + Vapor.

Inches H2O	GALLONS LIQUID	MSCF TOTAL	Inches H2O	GALLONS LIQUID	MSCF TOTAL
.64	0	20	5.6	1574	174
.7	1	20	5.7	1609	178
.8	7	21	5.8	1643	181
.9	18	22	5.9	1678	184
1	34	23	6	1712	188
1.1	53	25	6.1	1747	191
1.2	76	27	6.2	1781	195
1.3	102	30	6.3	1816	198
1.4	131	33	6.4	1850	201
1.5	162	36	6.5	1885	205
1.6	194	39	6.6	1919	208
1.7	228	42	6.7	1954	212
1.8	262	46	6.8	1989	215
1.9	297	49	6.9	2023	218
2	331	52	7	2058	222
2.1	366	56	7.1	2092	225
2.2	400	59	7.2	2127	228
2.3	435	63	7.3	2161	232
2.4	469	66	7.4	2196	235
2.5	504	69	7.5	2230	239
2.6	538	73	7.6	2265	242
2.7	573	76	7.7	2299	245
2.8	607	80	7.8	2334	249
2.9	642	83	7.9	2368	252
3	676	86	8	2403	256
3.1	711	90	8.1	2437	259
3.2	746	93	8.2	2472	262
3.3	780	96	8.3	2506	266
3.4	815	100	8.4	2541	269
3.5	849	103	8.5	2576	272
3.6	884	107	8.6	2610	276
3.7	918	110	8.7	2645	279
3.8	953	113	8.8	2679	283
3.9	987	117	8.9	2714	286
4	1022	120	9	2748	289
4.1	1056	124	9.1	2783	293
4.2	1091	127	9.2	2817	296
4.3	1125	130	9.3	2852	300
4.4	1160	134	9.4	2886	303
4.5	1194	137	9.5	2921	306
4.6	1229	140	9.6	2955	310
4.7	1263	144	9.7	2990	313
4.8	1298	147	9.73	3000	314
4.9	1332	151			
5	1367	154			
5.1	1402	157			
5.2	1436	161			
5.3	1471	164			
5.4	1505	168			
5.5	1540	171			
5.6	1574	174			

Sheet 1 of 1 07-31-2013

Appendix B: Boil-off simulation code

The boil-off simulation code used in this paper was released as open-source and is available at: https://github.com/LLNL/LH2Transfer

This code was developed and tested using MATLAB R2013b and REFPROP DLL version 9.1 for parahydrogen, on a laptop PC running on 64-bit Windows 10 Enterprise (2016), with an Intel Core -7-6600U CPU @ 2.60 GHz and a 16.0 GB RAM.

The simulation code consists of 9 MATLAB files that should be in the same folder:

- *runNominal.m* : runs the overall code
- *inputs_TrailerToDewar.m* : initializes the inputs and boundary conditions
- *LH_2Control.m* : controls the different steps of the fill process
- *LH_2Simulate.m* : solves the governing ordinary integro-differential equations using an ODE solver (odes15s)
- *Data_extraction.m* : post-processes output data
- *cylVtoH.m:* function used in the post-processing step. Converts volume of LH_2 in a horizontal cylinder to a height of fluid
- *gasFlow.m:* function used in the post-processing step. Calculates the flow rates (chocked or not) between 2 vessels.
- *vaporpressure.m:* function used in the post-processing step. Calculates vapor pressure (2 phases or not) based on temperature and density.
- *plotLH_2Data.m* : plots output data, in multiple separate figures

Running *runNominal.m* with the MATLAB software will solve governing equations and save the results in "output.txt", located in the same folder as the other files. Please refer to *runNominal.m* for the nomenclature of the output file.

Please not that package only works if a REFPROP subroutine compatible with MATLAB is installed on the computer. For linking REFPROP with MATLAB, make sure to follow instructions that can be found online, such as http://trc.nist.gov/refprop/LINKING/Linking.htm (*accessed 12/7/2017*). If running into issues with .dll from MATLAB, make sure you install REFPROP in "Program Files (x86)" and that the REFPRP64_thunk_pcwin64.dll is in that directory.